Coordination Chemistry Reviews 464 (2022) 214560

Contents lists available at ScienceDirect

Coordination Chemistry Reviews

journal homepage: www.elsevier.com/locate/ccr

Review

Nitrite reduction in bacteria: A comprehensive view of nitrite reductases

Stéphane Besson [a,b], M. Gabriela Almeida [c,d,*], Célia M. Silveira [e]

[a] Escola de Psicologia e Ciências da Vida, Departamento de Ciências da Vida, Universidade Lusófona de Humanidades e Tecnologias, Campo Grande, 1749-024 Lisboa, Portugal
[b] LAQV, REQUIMTE, Faculdade de Ciências e Tecnologia, Universidade NOVA de Lisboa, 2829-516 Monte de Caparica, Portugal
[c] UCIBIO, REQUIMTE, Faculdade de Ciências e Tecnologia, Universidade NOVA de Lisboa, 2829-516 Monte de Caparica, Portugal
[d] Centro de Investigação Interdisciplinar Egas Moniz (CiiEM), Instituto Universitário Egas Moniz, Campus Universitário, Quinta da Granja, 2829-511 Caparica, Portugal
[e] Instituto de Tecnologia Química e Biológica António Xavier, Universidade NOVA de Lisboa, Av. da República, 2780-157 Oeiras, Portugal

ARTICLE INFO

Article history:
Received 20 November 2021
Received in revised form 23 February 2022
Accepted 4 April 2022
Available online 26 April 2022

Dedicated to Prof. Isabel Moura and Prof. José J.G. Moura, in honor of their 70th birthday.

Keywords:
Nitrogen cycle
Dissimilatory nitrite reduction
Multiheme proteins
Copper centers

ABSTRACT

The last years have witnessed a steady increase of social and political awareness for the need of studying, monitoring, and controlling several anthropological activities that are dramatically impacting the environment and human health. The increasing turnover rates of the nitrogen cycle across the Planet are of major concern, so the understanding of the biological, chemical, and physical processes associated with the biogeochemical nitrogen cycle has been attracting the attention of several scientific disciplines. For many years, the primary focus has been the so-called "dissimilatory reduction of nitrate", which refers to the stepwise conversion of nitrate into molecular nitrogen, closely followed by the assimilatory nitrate reduction pathway, which allow nitrogen incorporation into biomolecules. The contribution of bioinorganic chemists to better understand the enzymology underlying these two branches of the *N*-cycle has been remarkable. The constant development of mechanistic, structural, and biological tools has been keeping this bioinorganic chemistry field very active, making it a highly relevant research area still today. In this paper, we review the state-of-the-art in both dissimilatory and assimilatory nitrite reducing enzymes, highlighting the structural peculiarities of the different metalloenzymes involved in this step.

Contents

* Corresponding author at: UCIBIO, REQUIMTE, Faculdade de Ciências e Tecnologia, Universidade NOVA de Lisboa, 2829-516 Monte de Caparica, Portugal.
E-mail address: mg.almeida@fct.unl.pt (M.G. Almeida).

https://doi.org/10.1016/j.ccr.2022.214560
0010-8545/

1. Introduction

The biogeochemical nitrogen cycle is the one most impacted by anthropogenic activities, such as food and energy production [1,2]. Globally, the nitrogen input to the environment has more than doubled over the last century, enhancing the losses of reactive nitrogen to the environment, with clear costs for the ecosystems, the chemistry of the atmosphere, and ultimately, for the climate change, and the human health [3,4]. The intensification of agriculture practices, in particular, has been responsible for the massive loading of fields with synthetic nitrogen fertilizers, such as ammonium nitrate. Almost 50% of these drains from the soils, contaminating land, surface, and groundwaters [5], which leads to a cascade of events that impact the environment, ranging from the eutrophication of water bodies and global acidification to the unbalance of the biogeochemical *N*-cycle [1].

Denitrification, a microbial process that accounts for the dissimilatory transformation of nitrate (NO_3^-) and nitrite (NO_2^-) into nitrogen (N_2), is thus directly perturbed. This important branch of the biological *N*-cycle is ubiquitous to terrestrial and aquatic ecosystems, either in marine and freshwater environments, including natural and intensively managed ecosystems. Denitrifying organisms include a wide range of bacteria, archaea and some fungi, which can use *N*-oxides in place of dioxygen as terminal electron acceptors in anaerobic respiration (energy release) [6]. Overall, the process relies on several *O*-abstraction reactions catalyzed by different metalloenzymes that sequentially convert nitrate → nitrite → nitric oxide → nitrous oxide → dinitrogen [7]. Although the majority of denitrified-*N* ends up as N_2, a small portion is lost to the atmosphere as chemically reactive (NO) or greenhouse (N_2O) gases [8]. It is interesting to note that many bacteria lack the last enzyme required to reduce nitrous oxide into molecular nitrogen [1,2,9].

The dissimilatory nitrate reduction to ammonia (DNRA), also known as **nitrate/nitrite ammonification**, is an alternative respiratory pathway used by fermentative bacteria for energy conservation under microaerophilic or anaerobic conditions. It is based on two steps only, representing a short circuit in the biological *N*-cycle; upon the conversion of nitrate into nitrite, the latter is directly reduced to ammonium (nitrate → nitrite → ammonium) [10,11].

Both denitrification and DNRA are catabolic pathways that can compete for nitrate utilization, depending on the microorganisms and the environmental conditions [9,11]. In carbon limiting media, nitrite accumulates and denitrification predominates, whereas under carbon-rich conditions, DNRA prevails [11].

The sequential reduction of nitrate into nitrite and ammonium can be also used by some bacteria for anabolic purposes in ammonium-limited environments. Collectively, the process of nitrate uptake, reduction to ammonium and incorporation into cellular biomass is known as nitrate assimilation [11]. Aside heterotrophic bacteria, assimilatory nitrate reduction is also carried out is by fungi, cyanobacteria, algae, and plants [12].

The recognized biological and environmental importance of bacterial nitrite reduction has driven extensive research on the structure and catalytic mechanisms of the participating enzymes for the last 50 years. In this review paper, focus will be given to the broad family of **nitrite reductases** (NiRs), a group of specialized enzymes in bacteria that either perform the one-electron reduction of nitrite to nitric oxide at the second step of the denitrification pathway Eq. (1), or catalyze the direct six-electron reduction of nitrite into ammonium Eq. (2), as a part of the DNRA branch or the assimilatory nitrate metabolism.

$$NO_2^- + 2H^+ + 1e^- \rightarrow NO + H_2O \quad (1)$$

$$NO_2^- + 8H^+ + 6e^- \rightarrow NH_4^+ + 2H_2O \quad (2)$$

The contribution of bioinorganic chemists to the understanding of the structural particularities of these metalloenzymes, as well as for the reaction mechanism underlying their catalytic activities has been remarkable.

Two different NO-forming nitrite reductases have been identified so far. According to the type of co-factors, they are designated as copper-containing nitrite reductase (NirK) and cytochrome cd_1 nitrite reductase (NirS). NirKs are composed of three identical subunits housing several copper centres, which can either work as electron transfer centers or as the catalytic site. NirS are homodimeric proteins, each subunit containing a *c*-type heme and the unique d_1 heme; the first acts as electron acceptor whereas the second is the catalytic center. As for the dissimilatory ammonia-forming nitrite reductases, they are all multiheme enzymes, generally known as cytochrome *c*-type NiRs (*cc*NiRs). The pentahemic NrfA is a homodimer, each subunit housing 5 hemes groups, while the octahemic nitrite reductase (ONR) is a homohexameric protein, each monomer presenting 8 different hemes. Regarding the assimilatory nitrite reductases (aNiRs), they are characterized for having an unusual siroheme group at the catalytic site. According to the physiological electron donor, they are classified as NAD(P)H-dependent nitrite reductases or ferredoxin-dependent nitrite reductases (FdNiRs), but the latter are mainly found in photosynthetic organisms such as cyanobacteria, algae, and plants.

The following sections will provide an in-depth description of each class of NiR, with special emphasis on the co-factors' features. Although aNiRs are less well characterized from the structural and mechanistic viewpoints, a brief description of this type of nitrite-metabolizing enzymes is also included in the last section of the manuscript.

2. Nitrite reduction to nitric oxide

2.1. Cytochrome cd_1 nitrite reductase

Cytochrome cd_1 (NirS) is one of two different types of dissimilatory nitrite reductases involved in the one-electron reduction of nitrite (NO_2^-) to nitric oxide (NO) as a part of the denitrification pathway of the biological cycle.

Cytochrome cd_1 structure from *Paracoccus pantotrophus* was elucidated in 1995 by Fülöp and coworkers [13]. The protein is an approximately 120 kDa homodimer, each subunit divided in a heme *c* containing domain and a heme d_1 containing domain (Fig. 1). The former is mostly made of α-helices, while the latter

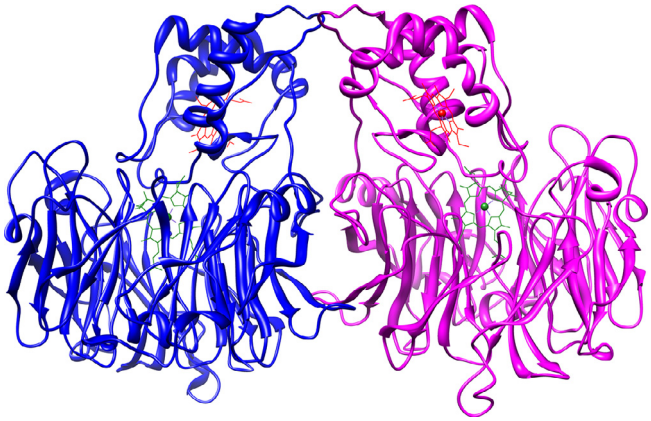

Fig. 1. Three-dimensional structure of *Paracoccus pantotrophus* oxidized cytochrome cd_1 (PDB: 1QKS) [13]. Subunits in different colours, heme *c* in red, heme d_1 in green. Molecular graphics and analyses performed with UCSF Chimera [16].

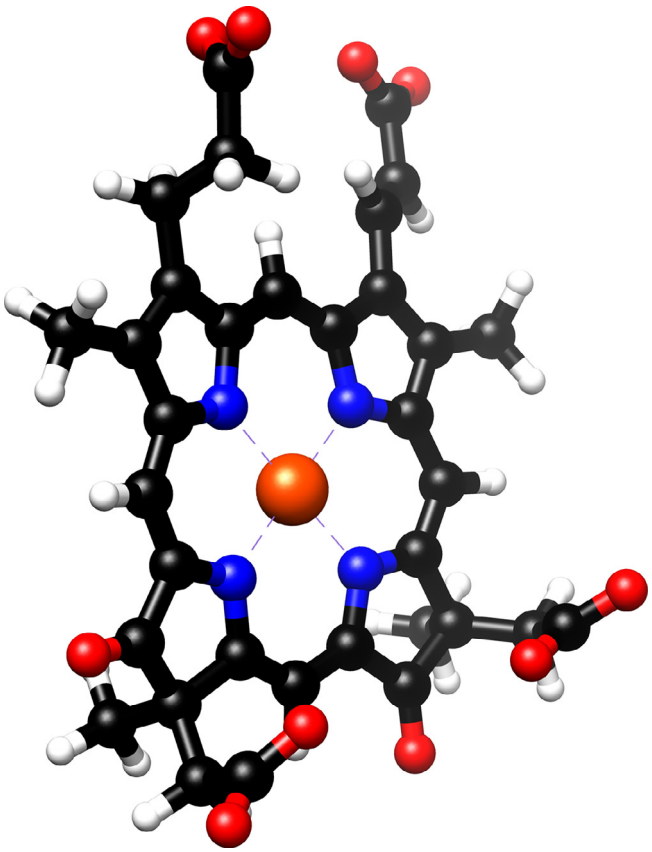

Fig. 2. Three-dimensional structure of heme d_1 (as extracted from cytochrome cd_1 structure PDB: 1QKS) [13]. Standard CPK color assignment. Molecular graphics and analyses performed with UCSF Chimera [16].

presents a larger β-propeller structure. So far, heme d_1 has only been encountered in nitrite reductases. Its structure was first confirmed by Chang and Wu in 1986 [14]: heme d_1 is a dioxo-isobacteriochlorin (Fig. 2) and, unlike heme *c*, it is not covalently linked to the protein. Apart from *P. pantotrophus*, the structure of this specific enzyme was determined from another bacterial species, *Pseudomonas aeruginosa* [15]. Although both proteins are similar, significant differences were observed regarding heme *c* domain structure and heme-coordination.

In *P. pantotrophus* nitrite reductase, heme *c* exhibits a His^{17}-His^{69} coordination in the oxidized state, shifting to a His^{69}-Met^{106} coordination upon reduction (Fig. 3) [17]. In the enzyme isolated from *P. aeruginosa*, however, heme *c* retains an unchanged His^{51}-Met^{88} coordination in both oxidation states [18], which is *hexa*-coordinated and low spin (LS) [19–22]. Heme d_1 is *hexa*-coordinated in the ferric state (His^{200}-Tyr^{25} and in a LS – high spin (HS) mixture in *P. pantotrophus* NirS, His^{182}-OH and LS for *P. aeruginosa* NirS), while ferrous heme d_1 is penta-coordinated with histidine as the only axial ligand, the sixth ligation remaining available for substrate binding [13,15,17,19–22]. Nurizzo and coworkers [23] suggested that heme d_1 reduction is responsible for heme *c* domain conformation changes since heme *c* reduction by itself does not seem to trigger any change. Substrate or product binding experiments in both enzymes led to the determination of nitrite-bound and NO-bound cytochrome cd_1 structures, thus confirming that heme d_1 is the catalytic site [17,18]. In *P. aeruginosa* NirS, an extended N-terminal arm wraps itself over the opposite subunit, interacting with both heme domains near their interface. This particular inter-monomer interaction, unobserved in *P. pantotrophus* NirS, appears to increase the dimer stability [15].

The cytochrome cd_1 dimer may not be the whole story: Terasaka and coworkers discovered that *P. aeruginosa* NirS tends to form a complex with membrane-integrated nitric oxide reductase, the next enzyme in the denitrification pathway, which reduces two NO molecules to nitrous oxide (N_2O) [24]. According to the authors, the existence of such a complex would explain why cytochrome cd_1, although water-soluble, would also consistently appear in the membrane fraction in smaller quantities. Physiologically, a strong cytochrome cd_1-NO interaction would provide to the denitrifier a means of minimizing nitric oxide cytotoxicity. The proximity between catalytic sites within the complex would allow NO to be consumed immediately upon production, thus limiting NO diffusion into the cell.

It should be emphasized that NirS biodiversity studies to date are far from being exhaustive. The increasing knowledge of prokaryotic genome sequences suggests that atypical NirS-like enzymes remain to be characterized. For instance, the sequence discovered in the genome of the crenarchaeota *Pyrobaculum aerophilum*, an organism known to grow on nitrogen oxides, does not possess the necessary cysteines to bind heme *c* in the N-terminal domain of the protein [25]. Although the gene product remains to be characterized, this fact implies that heme d_1 – mediated nitrite reduction may not always rely on intramolecular electron transfer (ET) from heme *c*.

Cytochrome cd_1 is a deep-green protein with a brownish tone, easily identifiable in chromatography columns [26]. Its UV–visible spectrum exhibits absorption bands that may be assigned to its very different hemes (Table 1). Heme *c* δ peak and heme d_1 γ peak appear as mere shoulders at approximately 360 nm and 460 nm, respectively. In almost all characterized cytochromes cd_1, heme *c* exhibits a split α peak, with 4 to 6 nm between absorption maxima; an exception would be the cytochrome cd_1 isolated from *Alcaligenes eutrophus* with a simple α peak reported for heme *c* [27]. Heme d_1 α band does not appear as a well-resolved peak and covers a wide wavelength interval. In *Pa. denitrificans* [28], this band even exhibits two maxima. While studying the NirS isolated from the closely related *P. pantotrophus*, Cheesman and co-workers [19] discovered that the peculiar form of this heme d_1 α band was the result of a LS/HS mixture. The relative proportions of both species are temperature-dependent and, upon lowering the temperature, the LS species becomes progressively dominant, with an absorption maximum at approximately 644 nm for the oxidized protein.

Low-temperature EPR spectra of oxidized cytochrome cd_1 show a rhombic signal for each LS heme (Table 2). For *Marinobacter hydrocarbonoclasticus* (formerly *Pseudomonas nautica*) cytochrome cd_1, the best resolution was obtained for a temperature of 10 K [26]. The assignment of each signal to a particular moiety was the result of an early work by Hill and Wharton on *P. aeruginosa* NirS [32]: following heme d_1 extraction, the remaining EPR signal could be assigned to heme *c*. Upon enzyme reduction with ascorbate or dithionite, both hemes become diamagnetic. However, reduced cytochrome cd_1 may react with nitrite to form a paramagnetic reduced heme d_1 – NO complex [26,33]. This NO adduct exhibits a complex signal with a hyperfine structure that may be simulated by introducing two different values of nitrogen hyperfine constants, thus confirming that the fifth ligand of heme d_1 is also a nitrogen, in agreement with published structures that show a histidine as this particular ligand [13,15]. For *M. hydrocarbonoclasticus* cytochrome cd_1, this signal was simulated with the following parameters: g_{max} = 2.055 (linewidth 5 mT), g_{med} = 1.990 (linewidth 0.56 mT, hyperfine constants A_1 = 2.6 mT and A_2 = 0.65 mT) and g_{min} = 1.945 (linewidth 5 mT) [26].

Midpoint redox potentials were determined in *M. hydrocarbonoclasticus* cytochrome cd_1 by redox titration under anaerobic

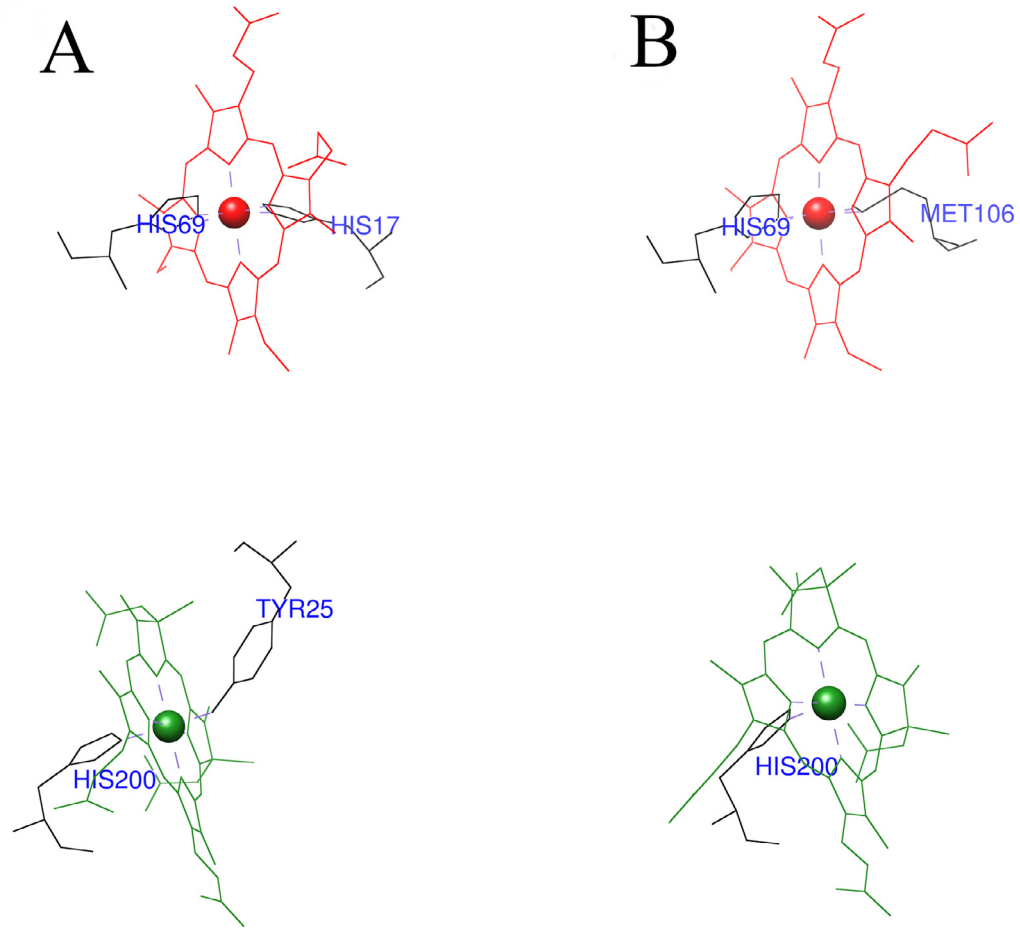

Fig. 3. Heme coordination in oxidized and fully reduced states of *Paracoccus pantotrophus* cytochrome cd_1 (PDB: 1QKS and 1AOF) [13,17]. Heme *c* in red, heme d_1 in green. A) Oxidized hemes; B) reduced hemes. Molecular graphics and analyses performed with UCSF Chimera [16].

Table 1
UV–visible absorption peaks of cytochrome cd_1 isolated from different sources.

	Heme *c* (nm)				Heme d_1 (nm)		
Biological source	δ	γ	β	α	γ	α	Reference
M. hydrocarbonoclasticus							
- oxidized	≈ 360	409	521	–	–	636	[26]
- reduced	-	416	521	548/552	460	629	
P. aeruginosa							
- oxidized	≈ 360	411	520	–	–	640	[29]
- reduced	-	417	520	548/554	456	650	
P. stutzeri							
- oxidized	≈ 360	411	525	–	–	641	[19,30]
- reduced	-	417	522	548/554	460	625–655	
P. denitrificans							
- oxidized		407	530	–	–	641/702	[28]
- reduced		417	522	548/553	460	630/655	
Thiobacillus denitrificans							
- oxidized	352	406.5	525			642	[31]
- reduced		418	523	549/553	460	650	

conditions [26]. Potentials of both hemes appear extremely close to each other: +249 mV (*c*) / +237 mV (d_1), +234 mV (*c*) / +199 mV (d_1) and + 245 mV (*c*) / +230 mV (d_1) at pH 6.6, 7.6 and 8.6, respectively. Similar values were observed in *Roseobacter denitrificans* (+240 mV (*c*) / +234 mV (d_1) at pH 7) [34] while almost no difference was reported for the *Ps. aeruginosa* enzyme (+288 mV or +294 mV (*c*) / 287 mV (d_1) at pH 7) [35,36].

2.2. Copper nitrite reductase

The second kind of nitrite reductase catalyzing the one-electron reduction of nitrite to nitric oxide, Eq. (1), in the denitrification pathway is the copper nitrite reductase (NirK).

In 1991, Godden and coworkers were able to resolve the three-dimensional structure of the enzyme isolated from the bacterium

Table 2
EPR parameters of oxidized cytochrome cd_1 isolated from different sources. ND - not determined

	Heme *c*			Heme d_1			
Biological source	g_z	g_y	g_x	g_z	g_y	g_x	Reference
M. hydrocarbonoclasticus	2.92	2.35	ND	2.51	2.33	1.67	[26]
P. aeruginosa	2.97	2.26	1.40	2.51	2.43	1.73	[20]
P. stutzeri	2.97	2.24	1.40	2.56	2.42	1.58	[19]
P. pantotrophus	3.05	ND	ND	2.52	2.19	1.84	[19]
Thiobacillus denitrificans	3.6	ND	ND	2.50	2.43	1.70	[31]

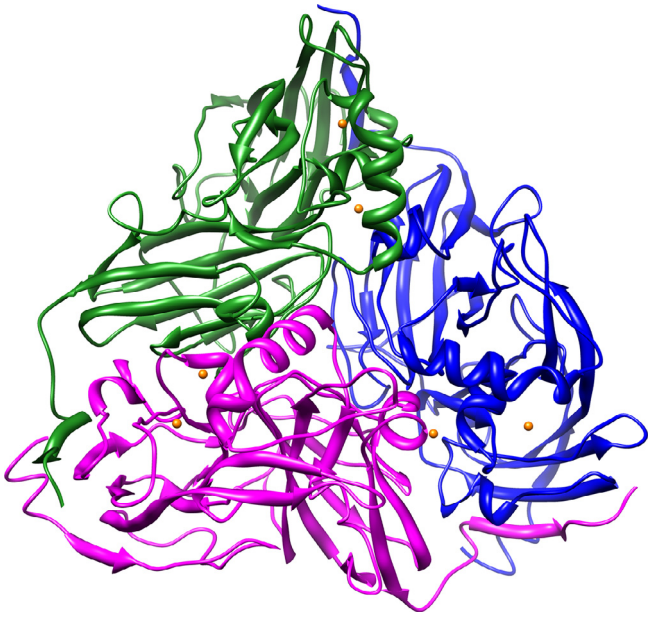

Fig. 4. Three-dimensional structure of *Alcaligenes faecalis* copper nitrite reductase (PDB: 1AS7) [38]. Subunits in different colors, copper ions in orange. Molecular graphics and analyses performed with UCSF Chimera [16].

Achromobacter cycloclastes [37]. Since then, the structures of a dozen homologous enzymes have been determined and published. NirK usually is a homotrimer, and each monomer, with a molecular mass of approximately 40 kDa, exhibits two distinct copper centers, a type 1 (CuI) and a type 2 (CuII) copper center (Fig. 4) [38]. In *A. cycloclastes* NirK, CuI is coordinated by two histidines, one cysteine and one methionine, while CuII is coordinated by three histidines and a solvent molecule [37]. CuI is nested within the monomer while CuII is encountered at the interface between monomers. In NirK, CuI was found to be responsible for the ET between the physiological electron donor and CuII, the catalytic center of the enzyme [39–42]. It must be noted that copper ions in NirK appear extremely labile during purification, storage or manipulation, and copper quantification usually yields values inferior to those expected from published structures [43,44]. Protein incubation with copper sulfate allows a partial regeneration of the enzyme copper content [44]. Some atypical NirKs were also described and their structure elucidated. *Thermus scotoductus* NirK presents three copper centers *per* monomer instead of two, the extra type 1 copper ion being settled in a distinct structural domain not encountered in "regular" NirK enzymes (Fig. 5) [45]. Another instance is the enzyme isolated from *Ralstonia pickettii*, where each monomer exhibits an extra heme-containing domain (Fig. 6) [46]. In both cases, the distance between this extra cofactor and CuI is compatible with ET and it is thus believed the additional domain may result from a gene fusion event with the sequence coding for the physiological electron donor [45,46].

Except for atypical NirKs, now regrouped in a third category where the extra metal center obviously contributes to the overall UV–visible spectrum, NirK enzymes are usually divided between blue and green NirKs, depending on the color of pure protein solution. While blue NirK exhibits a more intense absorption band at approximately 590 nm, green NirK shows a stronger absorption near 460 nm [47,48]. As an example, blue NirK isolated from *P. chlororaphis* DSM 50135 presents absorption maxima at 460 nm, 598 nm and a broader band near 780 nm for the native enzyme (oxidized). Absorption at the second peak is more intense with an A460nm/A598nm ratio equal to 0.496 [44]. This same ratio, however, approaches or exceeds 1 in green NirKs, like the

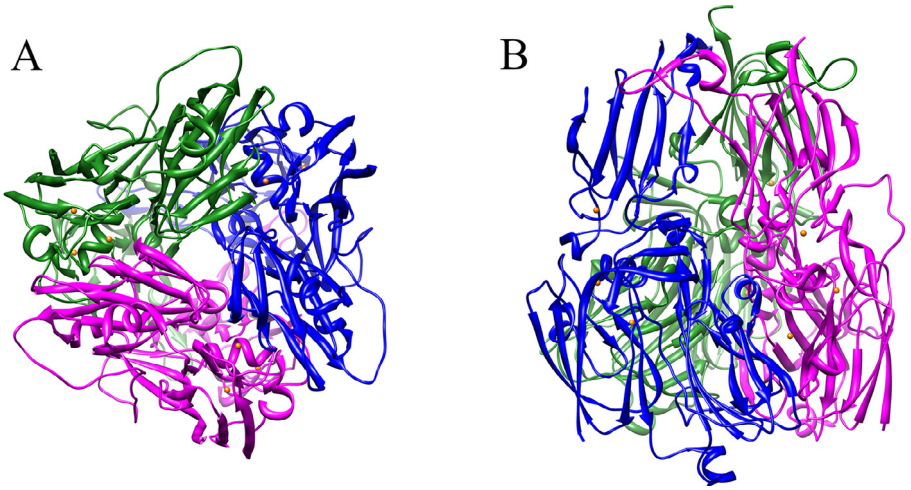

Fig. 5. Three-dimensional structure of *Thermus scotoductus* copper nitrite reductase (PDB: 6HBE) [45]. Subunits in different colours, copper ions in orange. A) View along symmetry axis; B) view perpendicular to symmetry axis. Molecular graphics and analyses performed with UCSF Chimera [16].

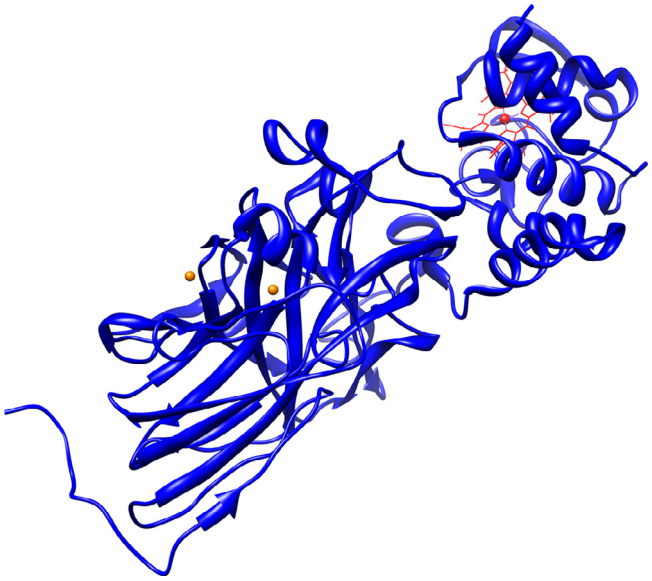

Fig. 6. Three-dimensional structure of monomer of *Ralstonia pickettii* copper nitrite reductase (PDB: 3ZIY) [46]. Copper ions in orange, heme *c* in red. Molecular graphics and analyses performed with UCSF Chimera [16].

nitrite reductase isolated from *Achromobacter cycloclastes* by Iwasaki and Matsubara, for which the A464nm/A590nm ratio is 1.3 [49]. Besides the peaks at 464 nm and 598 nm, the UV–visible spectrum of the *A. cycloclastes* enzyme also exhibits a shoulder around 400 nm and a broader band at 700 nm. Dodd and co-workers compared the three-dimensional structures of a blue NirK (from *A. xylosoxidans*) and a green NirK (from *A. faecalis*) in an attempt to identify structural differences responsible for the specific visible spectra. Cu-ligand bond lengths and ligand-Cu-ligand angles proved to be very similar in both structures, which led to the suggestion that observed spectral characteristics are due to very subtle differences in copper environment, for instance in the His-Cu-Met angle of CuI [43,47,48]. Both oxidized copper centers exhibit an EPR signal: as pointed out by Zumft in his 1997 review article, most NirKs exhibit a low temperature EPR spectrum resulting from the overlaying of two signals, one with a sharper hyperfine splitting (CuI) and another with a broader hyperfine splitting (CuII) [30]. In most NirKs isolated from bacteria, but also from the Archaea *Haloarcula marismortui* and the fungus *Fusarium oxysporum*, both EPR signals initially appear to be axial or near-axial, within the following range of values: $g_{\|}$ = 2.173–2.232 and $A_{\|}$ = 4.4–7.8 mT for CuI, $g_{\|}$ = 2.238–2.345 and $A_{\|}$ = 12.9–19.4 mT for CuII [30,39,43,44,50–60]. In some cases, however, selective CuI reduction allowed isolation of a CuII signal and hence facilitated the simulations of EPR signals overlaid in the native enzyme's spectrum. This led to the assignment of rhombic signals for CuII in *P. chlororaphis* NirK, with g_z = 2.350, g_y = 2.110, g_x = 2.040 and A_z = 10.7 mT [44] and for CuI in *Sinorhizobium meliloti* NirK, with g_z = 2.190, g_y = 2.062, g_x = 2.033 and A_z = 5.8 mT [52]. In addition, Deligeer and co-workers suggested, through spectrum simulations, that the EPR signal for CuI in *Hyphomicrobium denitrificans* NirK results from overlaying an axial and a rhombic signal [50]. Upon reduction, both copper centers become EPR-silent.

Midpoint redox potentials for CuI have been reported ranging from +224 to +298 mV, while the potentials for CuII are often lower, in the +108 to +260 mV range [44,61–65]. This difference is particularly dramatic in NirKs isolated from *P. chlororaphis* and *Sinorhizobium meliloti*. In the former, the observed values were +172 mV for CuII and 298 mV for CuI [44], while for the latter the values were +108 mV for CuII and +224 mV for CuI [61]. Since CuI is the ET moiety, and CuII is the catalytic site, such a difference in potential does not appear to favor ET from CuI to CuII. However, EPR studies of both enzymes in the presence of nitrite suggest that the binding of nitrite to CuII increases the cofactor's potential, thus allowing a more efficient ET from CuI [44,61].

3. Nitrite reduction to ammonium

3.1. Cytochrome c nitrite reductase

The multiple *c*-type heme-containing nitrite reductases (*cc*NiRs) handle the remarkable six-electron / eight-proton reaction of nitrite reduction to ammonium. These enzymes have been isolated from a variety of bacteria including sulfate reducers, e.g., *Desulfovibrio desulfuricans* ATCC27774 and *Desulfovibrio vulgaris* Hildenborough [66,67], entereobacteria, e.g., *Escherichia coli* [68], or purple sulfur bacteria, e.g., *Thialkalivibrio nitratireducens* and *Thioalkalivibrio paradoxus* [69,70]. *cc*NiRs are involved in the final step in the DNRA pathway, a process used by several anaerobic and facultative anaerobic bacteria to grow using nitrate and nitrite as terminal electron acceptors [30,71,72]. Identification of *cc*NiRs in organisms that cannot grow by nitrate ammonification, such as *D. vulgaris*, suggests their involvement in other cellular functions [73]. In fact, *cc*NiRs have been shown to take part in stress response and detoxification of nitrogen species [74–76]. These enzymes can reduce hydroxylamine and nitric oxide to ammonium, as well as nitric oxide to nitrous oxide, albeit at lower rates than nitrite [70,77–81]. Some *cc*NiRs, can also convert sulfite to sulfide in a six-electron reduction reaction [73,80,82], suggesting they can connect the nitrogen and sulfur cycles. Still, the physiological significance of *cc*NiR's sulfite reductase activity remains unclear as the expression of the enzyme is not induced in the presence of sulfite [75].

The *cc*NiRs identified so far are either pentahemic (also called NrfA, from the encoding gene nrf: nitrite reduction with formate) or octahemic enzymes (octahemic nitrite reductase, ONR). The homology between the two types is low [70], but all *cc*NiRs share several common structural features. The most striking characteristic of *cc*NiRs is the presence of a CXXCK heme *c* binding motif, in which lysine replaces the common histidine as the proximal heme iron ligand (CXXCH binding motif), and that thus far has only been identified in these enzymes [67,68,83–85]. This lysine-coordinated HS heme constitutes the active site (heme 1 in NrfA and heme 4 in ONR), with nitrite binding at the iron's distal coordination position. The remaining (four or seven) cofactors are LS, bis-histidine-coordinated *c*-type hemes involved in electron storage and transfer to the active site. The distal active site cavity of *cc*NiRs is lined by three strictly conserved residues (arginine, tyrosine and histidine), which contribute to the environment of positive electrostatic charge in the active site, facilitating nitrite binding and reduction. Substrate and product access channels that connect the active site and solvent are also found in all *cc*NiR structures [67,68,83–85]. They have opposite electrostatic charges, positive and negative for substrate and product channels, respectively, and are thought to contribute to the high activity of these enzymes by guiding the flow of NO_2^- and NH_4^+ molecules [83–86]. Calcium ions are also present in most *cc*NiR structures. A highly conserved site is found near the active site and is thought to play a role in maintaining its structure, contribute to the local positive electrostatic charge and facilitate proton transfer steps. The calcium ion is coordinated by conserved glutamate, tyrosine, lysine and glutamine residues and two water molecules [87–90]. In some *cc*NiRs a second calcium site has been identified, coordinated by the propionates of hemes 3 and 4 in NrfAs or hemes 6 and 7 in octahemic enzymes. It is thought to have a structural role [67,68,85,89]. Recently, a new sub-type of

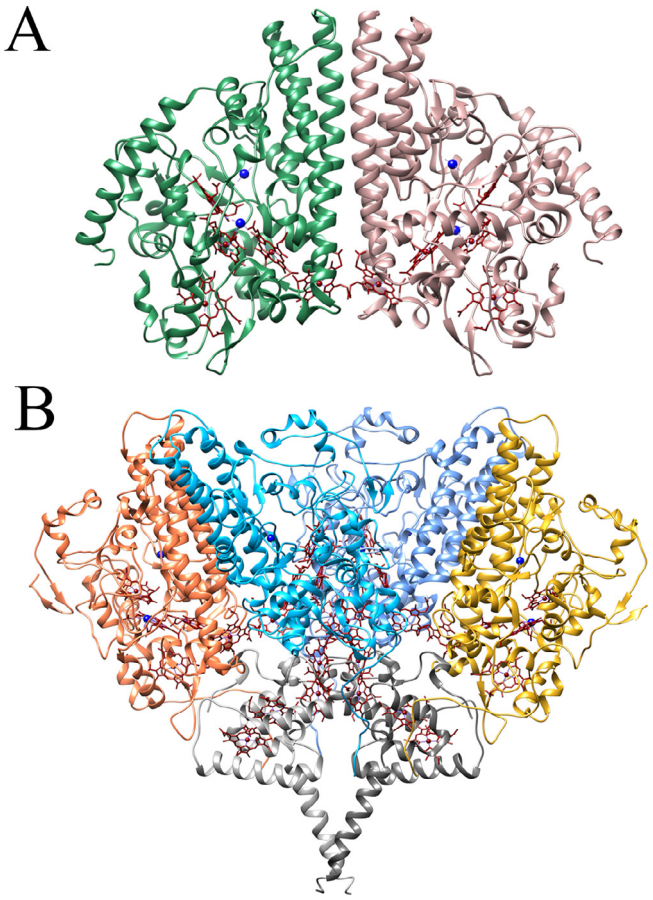

Fig. 7. Three-dimensional structures of A) *Escherichia coli* NrfA homodimer (PDB: 1GU6) [68] and B) *Desulfovibrio vulgaris* NrfA:NrfH 4:2 complex (PDB: 2J7A) [67]. NrfA subunits are shown in different colors and NrfH subunits are depicted in gray. Heme groups and calcium ions are represented in red and blue, respectively. Molecular graphics and analyses performed with UCSF Chimera [16].

pentahemic *cc*NiR that does not contain calcium ions in the structure has been identified in *Geobacter lovleyi*. A conserved arginine residue, essential for enzyme activity, is found instead in the region occupied by the active site calcium ion in other *cc*NiRs characterized to date [91].

The pentahemic *cc*NiRs, NrfA, were the first identified and are still the most well characterized. In early studies they were thought to have six, and later four hemes. The initial estimate was based on the analysis of iron content and spectroscopic data, while the later one was based on the amino acid sequence of the enzyme from *E. coli*, which revealed the presence of four typical *c*-type heme binding motifs (CXXCH) and the unique CXXCK motif. At the time, the CXXCK motif was not thought to bind a heme cofactor [77,92,93]. However, in the late 90s, mass spectroscopy studies [94] and the crystallographic structures of the enzymes from *Sulfurospirillum deleyanum* and *Wolinella succinogenes* [83,84] revealed the presence of five hemes in the structure of NrfA, including the lysine-coordinated heme active site.

NrfAs have been isolated as soluble periplasmic homodimers in γ-bacteria, such as *E. coli*, and in complexes with a membrane-bound tetraheme cytochrome *c*, NrfH, the electron donor to enzymes from ε and δ species (e.g., *W. succinogenes* and *D. desulfuricans*), usually in a 2NrfA: 1NrfH stoichiometry and likely as 4:2 biological units (Fig. 7) [66,67,95]. Notably, *G. lovleyi* NrfA was shown to remain as a monomer in solution, although it crystallizes as a dimer [91]. This enzyme belongs to a sub-type of NrfA, distinguished by the absence of calcium ions in the structure (cf. above).

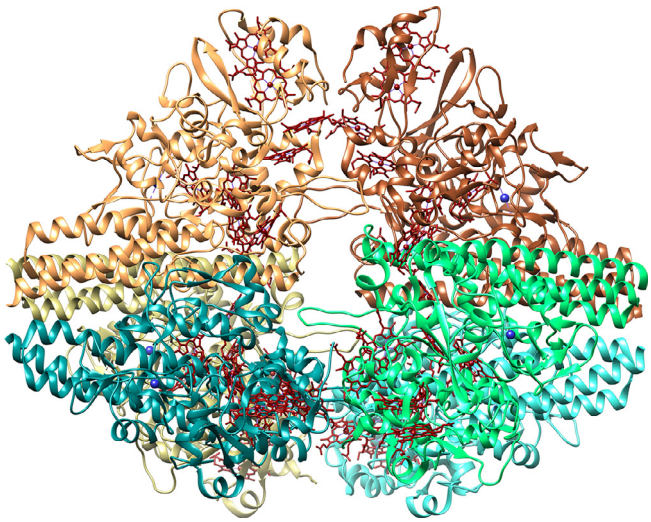

Fig. 8. Three-dimensional structure of *Thioalkalivibrio paradoxus* ONR hexamer (PDB: 3SXQ) [69]. Subunits are shown in different colors. Heme groups and calcium ions are represented in red and blue, respectively. Molecular graphics and analyses performed with UCSF Chimera [16].

Each NrfA subunit has a molecular weight of about 60 kDa and is organized in one compact domain with a mostly α-helical structure that envelops the five heme groups. Long α-helices define the interface with the second NrfA unit in the dimer, which is formed mainly via hydrophobic interactions. The five hemes are closely packed into parallel and perpendicular motifs, common to other multi-heme proteins, such as hydroxylamine oxidoreductase [83,84]. The arrangement accounts for efficient ET to the active site. Heme 5 interacts with its counterpart in the second NrfA monomer, as it is positioned at the dimer interface, thus guaranteeing facile ET between subunits (Fig. 7A). Owing to its exposure to the solvent, heme 2 is considered to be an electron entry point from electron donor partners [68]. Nonetheless, the structure of *D. vulgaris* NrfHA complex revealed heme edge-to-edge distances of 12.1 and 8.5 Å between hemes 2 and 5 in NrfA, respectively, and the nearest heme in NrfH structure, thus suggesting both heme 2 and 5 can accept electrons directly from the donor protein (Fig. 7B) [67].

The octahemic *cc*NiRs isolated so far originate from chromatiale purple sulfur bacteria, namely *T. nitratireducens* and *T. paradoxus* [69,70]. ONRs have homohexameric structures harboring 48 hemes in the crystalline state and in solution (Fig. 8). Each monomer is about 64 kDa and is organized in two domains. The catalytic domain contains five hemes, including the active site heme 4, which have identical arrangement to that found in NrfAs (Fig. 9, hemes 4 to 8 in ONR coincide with hemes 1 to 5 in NrfA); the overall three-dimensional structure is also similar to the α-helix rich NrfA conformation. The N-terminal domain hosts three additional hemes and displays a unique fold consisting of five α-helices and two β-sheets [69,85,96]. Besides the N-terminal domain, another distinctive feature of ONRs is the covalent bond between the conserved tyrosine in the active site's distal cavity and a nearby cysteine, which points towards the role of tyrosine as proton donor during the catalytic reaction and can explain the higher (*in vitro*) nitrite reduction activity of ONR in comparison to NrfA [97]. In addition, the product channel opens to the void interior space formed by the hexameric structure (Fig. 8), which can also account for higher activity [69].

The electron donor for NrfA of ε- and δ-proteobacteria (e.g., *W. succinogenes* and *D. desulfuricans*) is a membrane-bound tetra-heme cytochrome *c*, NrfH, with which the enzyme forms a

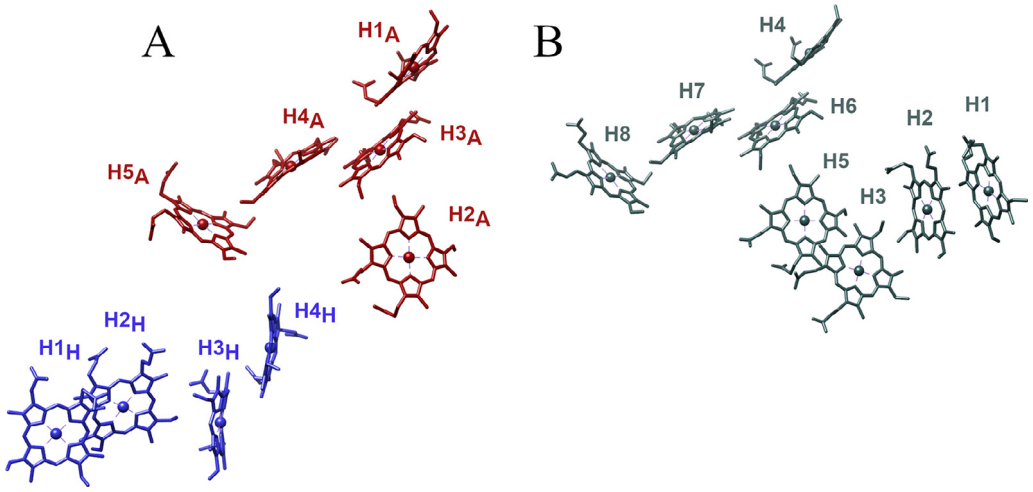

Fig. 9. Arrangement of hemes in A) *Desulfovibrio vulgaris* NrfA:NrfH complex (only one NrfA subunit is represented) and B) *Thioalkalivibrio paradoxus* ONR monomer. Heme groups are numbered according to the order of their binding motifs in the amino acid sequence. NrfA and NrfH hemes are labelled with Hx_A and Hx_H, respectively. Molecular graphics and analyses performed with UCSF Chimera [16].

heteroligomeric complex on the periplasmic membrane that allows the electron delivery from menaquinol to NrfA (4NrfA:2NrfH complex) [66,67]. In γ-bacteria, such as *E. coli*, electrons are delivered by soluble ET proteins, typically NrfB, a penta-heme cytochrome that interacts with the NrfD/NrfC membrane complex, believed to be involved in quinol oxidation and ET, respectively. The redox partners are thought to form a transient 2NrfA: 2NrfB complex in solution [81,95,98]. CymA, a membrane-bound tetra-heme cytochrome that serves as electron donor for several proteins, has been pointed as the electron donor to NrfA from *S. oneidensis*, a γ-proteobacteria that lacks genes encoding for NrfBCD/NrfH proteins [99,100]. As for the octahemic NiRs, thus far, their physiological electron donors have yet to be identified.

Analysis of the individual properties of the hemes has been challenging for any technique owing to the high number of hemes, overlapping features and interactions between them. The UV–visible spectra of *cc*NiRs display the typical features of *c*-type cytochromes [68,70,73,91,92,101]. In the oxidized, as isolated form, *D. vulgaris* NrfA spectrum reveals heme Soret band at 410 nm and Q band at 532 nm; in highly concentrated solutions, a charge transfer band is identified at ca. 630 nm, consistent with the presence of the HS heme active site. Reduction of the enzyme leads to a red-shift of the Soret band to 420 nm, while the α and β Q bands are found at 553 and 524 nm [73]. Only small differences are observed between enzymes from different organisms. Likewise, the EPR spectra of different *cc*NiRs are quite similar; note that only NrfAs have been characterized so far. The spectra are complex owing to the proximity of the heme groups and magnetic interactions between them. *E. coli* NrfA spectrum reveals a rhombic signal trio at $g_{x,y,z}$ = 2.92, 2.3 and 1.52 associated with the magnetically isolated heme 2. Features at g = 10.5 and 3.6 are both assigned to magnetically coupled HS heme 1 and the nearby LS heme 3, while a shoulder at g = 3.17 likely arises from the LS heme 4 and/or heme 5 [68]. The spectrum of the NrfHA complex from *D. vulgaris* also shows a set of resonances for heme 2 in NrfA ($g_{x,y,z}$ = 2.9, 2.27 and 1.5), while the features at g = 3.6 and 3.3 arise from coupled HS/LS hemes. The latter signals have been assigned to HS heme 1 in NrfA (coupled with heme 3) and the HS heme 1 in NrfH [67]. The signal found at g = 4.8 is also attributed to the NrfH subunit [66,73]; the feature is absent from the spectra of soluble periplasmic NrfA dimers like *E. coli*'s enzyme [68,102]. Partial reduction of the enzyme has enabled the isolation of the spectral features of the coupled hemes. The HS signal of the catalytic heme is usually identified at g ~ 6 [66,68,73].

The midpoint potentials of *cc*NiR hemes from different bacteria have been estimated through a variety of methods including EPR and UV–visible potentiometry as well as protein film voltammetry and surface enhanced Resonance Raman (SERR) spectroelectrochemistry [66,68,73,100,103–107]. The values reported span a broad range, +160 to −480 mV, nevertheless, the HS active site,

Table 3
Midpoint reduction potentials (E'_m) of NrfA and ONR isolated from different organisms. Heme groups (Hx) are numbered according to the order of their binging motifs in the amino acid sequence. EPR – electron paramagnetic resonance, SERR – surface-enhanced resonance Raman, CV – cyclic voltammetry, MCD – magnetic circular dichroism. * Value estimated from catalytic cyclic voltammetry measured at low nitrite concentration. † Values assigned to 1, 2 or 3 hemes (h).

Biological source / enzyme	Method	E'_m (mV vs. NHE)		Reference
		HS heme (catalytic site)	LS hemes (ET centers)	
D. desulfuricans / NrfA	Mossbauer and EPR potentiometry	−80	−50 (H2), ca. −480 (H3), ca. −400 (H4), +150 (H5)	[66]
	SERR spectroelectrochemistry	−50	–	[107]
	Electrochemistry (CV)	−200	–	[103]
E. coli / NrfA	EPR potentiometry	−107 (H1 + H3)	−37 (H2), −107 (H1 + H3), −323 (H4 + H5)	[68]
	MCD spectroelectrochemistry	−108	−20, −153, −206, −292	[106]
	UV–vis spectroelectrochemistry	−56	+22, −117, −189, −275	[106]
D. vulgaris / NrfA	UV–vis potentiometry	−110	+160, −5, −210	[73]
S. oneidensis / NrfA	UV–vis spectroelectrochemistry	−140	−62, −250, −283, −342	[100]
	Electrochemistry (CV)	−105	−36, −166, −230, −295	[100]
T. nitratireducens / ONR	UV–vis and MCD spectroelectrochemistry	<−100*	+100 (1 h), −80 (1 h), −200 (3 h), −370 (2 h)†	[104,105]

whose features can be more easily isolated from the multiple LS ET hemes, typically displays a midpoint potential around −100 mV (Table 3).

3.2. Siroheme nitrite reductase

Assimilatory nitrite reductases (aNiRs) are cytoplasmic enzymes that also catalyze the six-electron reduction of nitrite into ammonium Eq. (2), which is then incorporated into organic matter, the final step of the assimilatory nitrate reduction pathway. As opposed to the respiratory nitrate metabolisms, assimilatory nitrate reduction is inhibited by ammonium but is not affected by molecular oxygen [11,108]. As for ccNiRs, nitric oxide and hydroxylamine were proposed as reaction intermediates that are not released during catalysis [109].

As mentioned in Section 1, according to the electron donor specificity, aNiRs are classified as: *i)* ferredoxin-dependent NiRs (Fd-NiRs), which are characteristic of oxygenic photosynthetic organisms, either eukaryotic (algae and plants) and prokaryotic (cyanobacteria and the haloarchea *Haloferax mediterranei)*, and *ii)* reduced pyridine nucleotides-dependent enzymes (NAD(P)H-NiRs), typically found in non-photosynthetic organisms, such as fungi and heterotrophic bacteria, but also in the anoxygenic phototrophic bacterium *Rhodobacter capsulatus*. Aside the differences on the electron donor binding site, NAD(P)H-NiRs mainly differentiate from Fd-NiRs by the presence of an additional non-covalently bound FAD; both NAD(P)H and FAD molecules bind to the protein in an N-terminal extension that is not present in Fd-NiRs [12].

Due to its importance for the agriculture activities and for the environment, the nitrate assimilation pathway has been mainly studied in higher plants, fungi, and algae. Nevertheless, several physiological, genetic, and biochemical analysis have been carried out in some bacteria, including a few cyanobacteria, such as the unicellular *Synechococcus* and the filamentous *Anabaena*, the heterotrophic bacteria *Klebsiella oxytoca*, *Bacillus subtilis* and *Azotobacter vinelandii*, and the anoxygenic phototroph *R. capsulatus* [12]. The authors of these works have appointed distinct names to homologous genes codifying NAD(P)H-NiRs in different organisms, which created some confusion around the enzymes' designation [108]. While the great majority of Fd-NiRs are called NirA, the isoforms from the leaf and root of tobacco, among others, are designated as Nii [110]. For NAD(P)H-NiRs, we can find in the literature terms like NasA (e.g., *A. vinelandii* [111]), NasB (e.g., *R. capsulatus* [112], *Paracoccus denitrificans* [113]), NasDE (e.g., *B. subtilis* [114], *Bacillus megaterium* [115]), Nit-6 (e.g., *Neurospora crassa* [116]), and NirBD (e.g., *E. coli* [117], *Acidovorax wautersii* [118]). It is worth noting that the main role attributed to the *E. coli* NirBD is not aerobic nitrate assimilation; the enzyme is induced under anaerobic conditions, possibly to support fermentative ammonification and to contribute for nitrite detoxification during nitrate respiration [12,119].

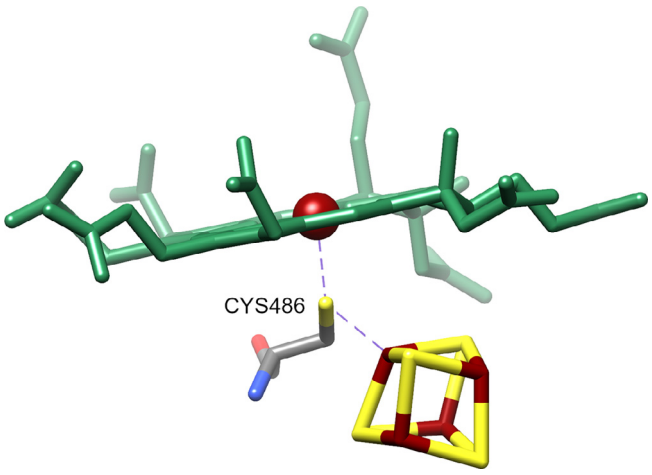

Fig. 10. Arrangement of siroheme and [4Fe–4S] center in spinach (*Spinacia oleracea*) nitrite reductase showing the common cysteine ligand (PDB: 2AKJ) [121]. Molecular graphics and analyses performed with UCSF Chimera [16].

The abbreviation *nir* has also been used to denote assimilatory nitrite reductases, which again is potentially confusing since the same abbreviation is being used to designate the respiratory nitrite reductases addressed in the previous sections [108]. To avoid any misunderstanding, herein we will strictly use the enzymes' designation based on the physiological redox partner, i.e., "ferredoxin-dependent" and "NAD(P)H dependent" NiRs.

Overall, Fd-NiRs and NAD(P)H-NiRs share considerable structural similarities. At the active site, they present a HS ferric siroheme, a complex heme derivative composed of an iron-containing isobacteriochlorin extensively substituted with carboxylic acid-containing side chains that is bridged to a tetranuclear [4Fe–4S] center through a common cysteine ligand [120,121] (Fig. 10). Electrons flow from the redox partner via this iron-sulfur cluster to the siroheme group [120], enabling the sequential reduction of nitrite at the distal position [110,118]. As explained below, two additional [2Fe–2S] centers are present in the NAD(P)H-NiRs from *Klebsiella* and *Bacillus*.

The siroheme co-factor was first identified in a NADPH-dependent sulfite reductase (SiR) from *E. coli*, which catalyzes the six-electron reduction of sulfite to hydrogen sulfide [122]. Curiously, *in vitro* assays have shown that SiRs can also perform the reduction of nitrite into ammonium while aNiRs can catalyze the sulfite reduction into sulfide. However, these activities should have no physiological relevance since the affinity of each enzyme for the alternative substrate is extremely low [123]. The primary structures of Fd-NiR and NAD(P)H-NiR have significant resemblances with the one from *E. coli* SiR, making this enzyme a good model for both classes of aNiRs [124]. The binding domains of the siroheam and iron-sulfur centers are highly conserved in SiRs and aNiRs. The same holds true for some peptide segments, such as the C-terminal amino acid sequence of bacterial NADH-NiRs, which show a high similarity with SiRs [12,108]. X-ray crystallographic structures of the siroheme-containing subunit from *E. coli* SiR [125,126] and some other organisms (e.g., *Mycobacterium tuberculosis* [127]) are available. However, high resolution crystal structures of Fd-NiRs are scarce and they all have a plant origin (spinach [121] and tobacco [110]). To the best of our knowledge, no three-dimensional structure of a NAD(P)H-NiR was published so far. Therefore, since the focus of this review manuscript is bacterial nitrite reductases, no three-dimensional description of these proteins could be made here.

Regarding the subunit composition, Fd-NiRs show a homogeneous pattern, i.e., they are all described as monomeric proteins with a molecular weight between 60 and 70 kDa [128]. On the contrary, bacterial NAD(P)H-NiR reductases show diverse configurations, ranging from a single subunit, such as that of *K. oxytoca*, or a heterodimer containing a large catalytic subunit of 90–105 kDa, and a small subunit of 45–50 kDa, as found in *B. subtilis* [115,129]. In this case, besides the siroheme, [4Fe–4S] and FAD groups, two additional [2Fe–2S] clusters are found in the catalytic subunit. Furthermore, the fungal NAD(P)H-NiR from *N. crassa* appears to be a homodimer composed of two 127 kDa subunits [116].

One should emphasize that over the last decades, most of the works regarding aNiRs in general, and NAD(P)H-NiRs, in particular, have preferentially addressed the biological aspects of nitrate assimilation, looking at the regulation of genes expression and cells adaptation. So, if compared to their counterpart dissimilatory

enzymes, bacterial aNiRs are poorly characterized from the structural and mechanistic standpoints. Some biochemical and spectroscopic studies were carried out during 1970–80 but since then, SiRs enzymes have attracted much greater attention from the scientific community. A large number of studies was focused on the spinach Fd-NiR enzyme but, in the absence of detailed data on bacterial aNiRs, we will assume that the polypeptide environment does not affect the structural and spectroscopic (UV–visible, EPR, Resonance Raman) properties of the inorganic cofactors much, and we will now summarize the main results obtained with this specific enzyme.

The spinach Fd-NiR is purified nearly all in its oxidized form [130] (reddish-brown in color), showing absorption peaks in the UV–visible spectrum at 278, 390 (siroheme Soret band), and 573 nm, with a ratio A_{390}/A_{278} of 0.5 [131]. Once fully reduced, the optical absorption spectrum shows peaks at 412, 549 and 604 nm [132].

In the "as isolated" enzyme form, the siroheme is in a HS ferric state, with the central Fe(III) hexa-coordinated to a weakly bound ligand (possibly a water molecule or a phosphate ion from the buffer) in the distal position, and to a cysteinyl sulfur (Cys^{486}) in the proximal position [121] that links the siroheme group to the $[4Fe–4S]^{2+}$ cluster (Fig. 10). Despite being magnetically coupled, the two redox centers respond independently in both spectroelectrochemical titrations and cyclic voltammetry: the estimated midpoint potentials (E_m) for the siroheme and iron-sulfur cluster are −290 mV and −370 mV, respectively [132]. The EPR spectrum of the oxidized enzyme shows three peaks with *g* values of 6.78, 5.17, and 1.98, which were assigned to a HS ferric heme [130]. The iron cluster has shown to be EPR-silent (S = 0). Upon nitrite binding, the enzyme-substrate complex becomes fully EPR-silent, and the electronic spectrum changes some features, denoting the ferric heme's transition from high-spin to low-spin [133].

4. Conclusion

Dissimilatory NiRs (dNiRs) are key enzymes in two branches of the biological nitrogen cycle. According to the product formed, they can be classified as nitric oxide- or ammonium-forming nitrite reductases. Despite catalyzing the same reaction, they are notably different from the structural and mechanistic standpoints, each one presenting a different set of metallic co-factors. Accordingly, we can find in Nature three different dNiRs classes, the cytochrome cd_1-NiRs, the copper-containing NiRs, and the multi-heme cytochrome *c* NiRs. A fourth class of enzymes is found in aNiRs, which present a siroheme at the active site. They convert nitrite into ammonium for anabolic purposes. The in-depth characterization of these metalloenzymes over the years has delivered important data that has been used in different fields, ranging from microbiology, bioremediation, biotechnology, and biosensors, among others.

Declaration of Competing Interest

The authors declare that they have no known competing financial interests or personal relationships that could have appeared to influence the work reported in this paper.

Acknowledgements

The authors acknowledge the support of the research centers Applied Molecular Biosciences Unit-UCIBIO, which is financed by national funds from FCT/MCTES (UID/Multi/04378/2013) and co-financed by the ERDF under the PT2020 Partnership Agreement (POCI-01-0145-FEDER-007728), and Centro de investigação interdisciplinar Egas Moniz – CiiEM (project IDB/04585/2020). CMS acknowledges support from Project LISBOA-01-0145-FEDER-007660 (Microbiologia Molecular, Estrutural e Celular) funded by FEDER funds through COMPETE2020 – Programa Operacional Competitividade e Internacionalização (POCI) and by national funds through FCT – Fundação para a Ciência e a Tecnologia and from PTDC/BIA-BFS/31026/2017 project funded by FCT.

References

[1] J.N. Galloway, E.B. Cowling, Reactive nitrogen and the world: 200 years of change, Ambio 31 (2002) 64–71, https://doi.org/10.1579/0044-7447-31.2.64.
[2] R.M. Martínez-Espinosa, J.A. Cole, D.J. Richardson, N.J. Watmough, Enzymology and ecology of the nitrogen cycle, Biochem. Soc. Trans. 39 (2011) 175–178, https://doi.org/10.1042/BST0390175.
[3] J.W. Erisman, J.N. Galloway, S. Seitzinger, A. Bleeker, N.B. Dise, A.M.R. Petrescu, A.M. Leach, W. de Vries, Consequences of human modification of the global nitrogen cycle, Philos. Trans. R. Soc. Lond. B Biol. Sci. 368 (2013) 20130116, https://doi.org/10.1098/rstb.2013.0116.
[4] D. Fowler, M. Coyle, U. Skiba, M.A. Sutton, J.N. Cape, S. Reis, L.J. Sheppard, A. Jenkins, B. Grizzetti, J.N. Galloway, P. Vitousek, A. Leach, A.F. Bouwman, K. Butterbach-Bahl, F. Dentener, D. Stevenson, M. Amann, M. Voss, The global nitrogen cycle in the twenty-first century, Philos. Trans. R. Soc. Lond. B Biol. Sci. 368 (2013) 20130164, https://doi.org/10.1098/rstb.2013.0164.
[5] S. Singh, A.G. Anil, V. Kumar, D. Kapoor, S. Subramanian, J. Singh, P.C. Ramamurthy, Nitrates in the environment: A critical review of their distribution, sensing techniques, ecological effects and remediation, Chemosphere 287 (2022), https://doi.org/10.1016/j.chemosphere.2021.131996 131996.
[6] S.E. Jorgensen, B.D. Fath, Denitrification, in: S.E. Jorgensen, B.D. Fath (Eds.), Encyclopedia of Ecology, Elsevier, 2008, pp. 866–871.
[7] D.J. Richardson, Bacterial respiration: a flexible process for a changing environment, Microbiology 146 (Pt 3) (2000) 551–571, https://doi.org/10.1099/00221287-146-3-551.
[8] L.R. Bakken, L. Bergaust, B. Liu, A. Frostegård, Regulation of denitrification at the cellular level: a clue to the understanding of N2O emissions from soils, Philos. Trans. R. Soc. Lond. B Biol. Sci. 367 (2012) 1226–1234, https://doi.org/10.1098/rstb.2011.0321.
[9] S. Durand, M. Guillier, Transcriptional and post-transcriptional control of the nitrate respiration in bacteria, Front. Mol. Biosci. 8 (2021), https://doi.org/10.3389/fmolb.2021.667758 667758.
[10] J.A. Cole, C.M. Brown, Nitrite reduction to ammonia by fermentative bacteria: A short circuit in the biological nitrogen cycle, FEMS Microbiol. Lett. 7 (1980) 65–72, https://doi.org/10.1111/j.1574-6941.1980.tb01578.x.
[11] R.M. Maier, Biogeochemical Cycling, Environmental Microbiology, Elsevier, 2015, pp. 339–373.
[12] C. Moreno-Vivián, E. Flores, Nitrate Assimilation in Bacteria, in: Biology of the Nitrogen Cycle, Elsevier, 2007: pp. 263–282.
[13] V. Fülöp, J.W. Moir, S.J. Ferguson, J. Hajdu, The anatomy of a bifunctional enzyme: structural basis for reduction of oxygen to water and synthesis of nitric oxide by cytochrome cd_1, Cell 81 (1995) 369–377, https://doi.org/10.1016/0092-8674(95)90390-9.
[14] C.K. Chang, W. Wu, The porphinedione structure of heme d1. Synthesis and spectral properties of model compounds of the prosthetic group of dissimilatory nitrite reductase, J. Biol. Chem. 261 (19) (1986) 8593–8596.
[15] D. Nurizzo, M.C. Silvestrini, M. Mathieu, F. Cutruzzolà, D. Bourgeois, V. Fülöp, J. Hajdu, M. Brunori, M. Tegoni, C. Cambillau, N-terminal arm exchange is observed in the 2.15 Å crystal structure of oxidized nitrite reductase from *Pseudomonas aeruginosa*, Structure 5 (1997) 1157–1171, https://doi.org/10.1016/s0969-2126(97)00267-0.
[16] E.F. Pettersen, T.D. Goddard, C.C. Huang, G.S. Couch, D.M. Greenblatt, E.C. Meng, T.E. Ferrin, UCSF Chimera-a visualization system for exploratory research and analysis, J. Comput. Chem. 25 (2004) 1605–1612, https://doi.org/10.1002/jcc.20084.
[17] P.A. Williams, V. Fülöp, E.F. Garman, N.F. Saunders, S.J. Ferguson, J. Hajdu, Haem-ligand switching during catalysis in crystals of a nitrogen-cycle enzyme, Nature 389 (1997) 406–412, https://doi.org/10.1038/38775.
[18] D. Nurizzo, F. Cutruzzolà, M. Arese, D. Bourgeois, M. Brunori, C. Cambillau, M. Tegoni, Conformational changes occurring upon reduction and NO binding in nitrite reductase from *Pseudomonas aeruginosa*, Biochemistry 37 (1998) 13987–13996, https://doi.org/10.1021/bi981348y.
[19] M.R. Cheesman, S.J. Ferguson, J.W. Moir, D.J. Richardson, W.G. Zumft, A.J. Thomson, Two enzymes with a common function but different heme ligands in the forms as isolated. Optical and magnetic properties of the heme groups in the oxidized forms of nitrite reductase, cytochrome cd_1, from *Pseudomonas stutzeri* and *Thiosphaera pantotropha*, Biochemistry 36 (1997) 16267–16276, https://doi.org/10.1021/bi971677a.
[20] B.B. Muhoberac, D.C. Wharton, Electron paramagnetic resonance study of the interaction of some anionic ligands with oxidized *Pseudomonas* cytochrome oxidase, J. Biol. Chem. 258 (1983) 3019–3027, https://doi.org/10.1016/s0021-9258(18)32823-0.
[21] R. Timkovich, M.S. Cork, Magnetic susceptibility measurements on *Pseudomonas* cytochrome cd_1, Biochim. Biophys. Acta 742 (1983) 162–168, https://doi.org/10.1016/0167-4838(83)90372-2.

[22] T.A. Walsh, M.K. Johnson, C. Greenwood, D. Barber, J.P. Springall, A.J. Thomson, Some magnetic properties of *Pseudomonas* cytochrome oxidase, Biochem. J. 177 (1979) 29–39, https://doi.org/10.1042/bj1770029.
[23] D. Nurizzo, F. Cutruzzolà, M. Arese, D. Bourgeois, M. Brunori, C. Cambillau, M. Tegoni, Does the reduction of *c* heme trigger the conformational change of crystalline nitrite reductase?, J Biol. Chem. 274 (1999) 14997–15004, https://doi.org/10.1074/jbc.274.21.14997.
[24] E. Terasaka, K. Yamada, P.-H. Wang, K. Hosokawa, R. Yamagiwa, K. Matsumoto, S. Ishii, T. Mori, K. Yagi, H. Sawai, H. Arai, H. Sugimoto, Y. Sugita, Y. Shiro, T. Tosha, Dynamics of nitric oxide controlled by protein complex in bacterial system, Proc. Natl. Acad. Sci. U.S.A. 114 (2017) 9888–9893, https://doi.org/10.1073/pnas.1621301114.
[25] S.T. Fitz-Gibbon, H. Ladner, U.-J. Kim, K.O. Stetter, M.I. Simon, J.H. Miller, Genome sequence of the hyperthermophilic crenarchaeon *Pyrobaculum aerophilum*, Proc. Natl. Acad. Sci. U.S.A. 99 (2002) 984–989, https://doi.org/10.1073/pnas.241636498.
[26] S. Besson, C. Carneiro, J.J. Moura, I. Moura, G. Fauque, A cytochrome cd_1-type nitrite reductase isolated from the marine denitrifier *Pseudomonas nautica* 617: purification and characterization, Anaerobe 1 (1995) 219–226, https://doi.org/10.1006/anae.1995.1021.
[27] R. Sann, S. Kostka, B. Friedrich, A cytochrome cd_1-type nitrite reductase mediates the first step of denitrification in *Alcaligenes eutrophus*, Arch. Microbiol. 161 (1994) 453–459, https://doi.org/10.1007/bf00307765.
[28] R. Timkovich, R. Dhesi, K.J. Martinkus, M.K. Robinson, T.M. Rea, Isolation of *Paracoccus denitrificans* cytochrome cd_1: comparative kinetics with other nitrite reductases, Arch. Biochem. Biophys. 215 (1982) 47–58, https://doi.org/10.1016/0003-9861(82)90277-6.
[29] M.C. Silvestrini, S. Falcinelli, I. Ciabatti, F. Cutruzzolà, M. Brunori, *Pseudomonas aeruginosa* nitrite reductase (or cytochrome oxidase): an overview, Biochimie 76 (1994) 641–654, https://doi.org/10.1016/0300-9084(94)90141-4.
[30] W.G. Zumft, Cell biology and molecular basis of denitrification, Microbiol. Mol. Biol. Rev. 61 (1997) 533–616, https://doi.org/10.1128/mmbr.61.4.533-616.1997.
[31] B.H. Huynh, M.C. Lui, J.J. Moura, I. Moura, P.O. Ljungdahl, E. Münck, W.J. Payne, H.D. Peck, D.V. DerVartanian, J. LeGall, Mössbauer and EPR studies on nitrite reductase from *Thiobacillus denitrificans*, J. Biol. Chem. 257 (16) (1982) 9576–9581.
[32] K.E. Hill, D.C. Wharton, Reconstitution of the apoenzyme of cytochrome oxidase from *Pseudomonas aeruginosa* with heme d_1 and other heme groups, J. Biol. Chem. 253 (1978) 489–495, https://doi.org/10.1016/s0021-9258(17)38236-4.
[33] M.C. Silvestrini, M.G. Tordi, G. Musci, M. Brunori, The reaction of *Pseudomonas* nitrite reductase and nitrite. A stopped-flow and EPR study, J. Biol. Chem. 265 (20) (1990) 11783–11787.
[34] M. Doi, Y. Shioi, M. Morita, K. Takamiya, Two types of cytochrome cd_1 in the aerobic photosynthetic bacterium, *Erythrobacter* sp. OCh 114, Eur. J. Biochem. 184 (1989) 521–527, https://doi.org/10.1111/j.1432-1033.1989.tb15045.x.
[35] S.A. Schichman, H.B. Gray, Kinetics of the anaerobic reduction of ferricytochrome cd_1 by $Fe(EDTA)^{2-}$. Evidence for bimolecular and intramolecular electron transfers to the d_1 hemes, J. Am. Chem. Soc. 103 (1981) 7794–7795, https://doi.org/10.1021/ja00416a020.
[36] M.C. Silvestrini, M.G. Tordi, A. Colosimo, E. Antonini, M. Brunori, The kinetics of electron transfer between *Pseudomonas aeruginosa* cytochrome c_{551} and its oxidase, Biochem. J. 203 (1982) 445–451, https://doi.org/10.1042/bj2030445.
[37] J.W. Godden, S. Turley, D.C. Teller, E.T. Adman, M.Y. Liu, W.J. Payne, J. LeGall, The 2.3 angstrom X-ray structure of nitrite reductase from *Achromobacter cycloclastes*, Science 253 (5018) (1991) 438–442.
[38] M.E.P. Murphy, S. Turley, E.T. Adman, Structure of nitrite bound to copper-containing nitrite reductase from *Alcaligenes faecalis*: Mechanistic implications, J. Biol. Chem. 272 (1997) 28455–28460, https://doi.org/10.1074/jbc.272.45.28455.
[39] Z.H. Abraham, D.J. Lowe, B.E. Smith, Purification and characterization of the dissimilatory nitrite reductase from *Alcaligenes xylosoxidans* subsp. *xylosoxidans* (N.C.I.M.B. 11015): evidence for the presence of both type 1 and type 2 copper centres, Biochem. J. 295 (1993) 587–593. 10.1042/bj2950587.
[40] M. Kukimoto, M. Nishiyama, M.E. Murphy, S. Turley, E.T. Adman, S. Horinouchi, T. Beppu, X-ray structure and site-directed mutagenesis of a nitrite reductase from *Alcaligenes faecalis* S-6: roles of two copper atoms in nitrite reduction, Biochemistry 33 (1994) 5246–5252, https://doi.org/10.1021/bi00183a030.
[41] E. Libby, B.A. Averill, Evidence that the type 2 copper centers are the site of nitrite reduction by *Achromobacter cycloclastes* nitrite reductase, Biochem. Biophys. Res. Commun. 187 (1992) 1529–1535, https://doi.org/10.1016/0006-291x(92)90476-2.
[42] S. Suzuki, T. Kohzuma, K. Deligeer, N. Yamaguchi, S. Nakamura, K. Shidara, S.T. Kobayashi, Pulse radiolysis studies on nitrite reductase from *Achromobacter cycloclastes* IAM 1013: Evidence for intramolecular electron transfer from type 1 Cu to type 2 Cu, J. Am. Chem. Soc. 116 (1994) 11145–11146, https://doi.org/10.1021/ja00103a035.
[43] F. Cutruzzolà, Bacterial nitric oxide synthesis, Biochim. Biophys. Acta Bioenerg. 1411 (1999) 231–249, https://doi.org/10.1016/s0005-2728(99)00017-1.
[44] D. Pinho, S. Besson, C.D. Brondino, B. de Castro, I. Moura, Copper-containing nitrite reductase from *Pseudomonas chlororaphis* DSM 50135, Eur. J. Biochem. 271 (2004) 2361–2369, https://doi.org/10.1111/j.1432-1033.2004.04155.x.
[45] D.J. Opperman, D.H. Murgida, S.D. Dalosto, C.D. Brondino, F.M. Ferroni, A three-domain copper-nitrite reductase with a unique sensing loop, IUCrJ 6 (2019) 248–258, https://doi.org/10.1107/S2052252519000241.
[46] S.V. Antonyuk, C. Han, R.R. Eady, S.S. Hasnain, Structures of protein-protein complexes involved in electron transfer, Nature 496 (2013) 123–126, https://doi.org/10.1038/nature11996.
[47] F.E. Dodd, J. Van Beeumen, R.R. Eady, S.S. Hasnain, X-ray structure of a blue-copper nitrite reductase in two crystal forms. The nature of the copper sites, mode of substrate binding and recognition by redox partner, J. Mol. Biol. 282 (1998) 369–382. 10.1006/jmbi.1998.2007.
[48] T. Inoue, M. Gotowda, K. Deligeer, K. Kataoka, S. Yamaguchi, H. Suzuki, M. Watanabe, Y.K. Gohow, Type 1 Cu structure of blue nitrite reductase from *Alcaligenes xylosoxidans* GIFU 1051 at 2.05 A resolution: comparison of blue and green nitrite reductases, J. Biochem. 124 (1998) 876–879, https://doi.org/10.1093/oxfordjournals.jbchem.a022201.
[49] H. Iwasaki, T. Matsubara, A nitrite reductase from *Achromobacter cycloclastes*, J. Biochem. 71 (1972) 645–652, https://doi.org/10.1093/oxfordjournals.jbchem.a129810.
[50] Deligeer, R. Fukunaga, K. Kataoka, K. Yamaguchi, K. Kobayashi, S. Tagawa, S. Suzuki, Spectroscopic and functional characterization of Cu-containing nitrite reductase from *Hyphomicrobium denitrificans* A3151, J. Inorg. Biochem. 91 (1) (2002) 132–138.
[51] G. Denariaz, W.J. Payne, J. LeGall, The denitrifying nitrite reductase of *Bacillus halodenitrificans*, Biochim. Biophys. Acta Bioenerg. 1056 (1991) 225–232, https://doi.org/10.1016/s0005-2728(05)80053-2.
[52] F.M. Ferroni, S.A. Guerrero, A.C. Rizzi, C.D. Brondino, Overexpression, purification, and biochemical and spectroscopic characterization of copper-containing nitrite reductase from *Sinorhizobium meliloti*, Study of the interaction of the catalytic copper center with nitrite and NO, J. Inorg. Biochem. 114 (2012) (2011) 8–14, https://doi.org/10.1016/j.jinorgbio.2012.04.016.
[53] H. Iwasaki, S. Noji, S. Shidara, *Achromobacter cycloclastes* nitrite reductase. The function of copper, amino acid composition, and ESR spectra, J. Biochem. 78 (1975) 355–361, https://doi.org/10.1093/oxfordjournals.jbchem.a130915.
[54] T. Kakutani, H. Watanabe, K. Arima, T. Beppu, A blue protein as an inactivating factor for nitrite reductase from *Alcaligenes faecalis* strain S-6, J. Biochem. 89 (1981) 463–472, https://doi.org/10.1093/oxfordjournals.jbchem.a133221.
[55] M. Kobayashi, H. Shoun, The copper-containing dissimilatory nitrite reductase involved in the denitrifying system of the fungus *Fusarium oxysporum*, J. Biol. Chem. 270 (1995) 4146–4151, https://doi.org/10.1074/jbc.270.8.4146.
[56] K. Kondo, K. Yoshimatsu, T. Fujiwara, Expression, and molecular and enzymatic characterization of Cu-containing nitrite reductase from a marine ammonia-oxidizing gamma-proteobacterium, *Nitrosococcus oceani*, Microbes Environ. 27 (2012) 407–412, https://doi.org/10.1264/jsme2.me11310.
[57] W.P. Michalski, D.J.D. Nicholas, Molecular characterization of a copper-containing nitrite reductase from *Rhodopseudomonas sphaeroides forma* sp. *denitrificans*, Biochim. Biophys. Acta. 828 (1985) 130–137, https://doi.org/10.1016/0167-4838(85)90048-2.
[58] D.J. Miller, D.J.D. Nicholas, Characterization of a soluble cytochrome oxidase/nitrite reductase from *Nitrosomonas europaea*, Microbiology 131 (1985) 2851–2854, https://doi.org/10.1099/00221287-131-10-2851.
[59] H. Ichiki, Y. Tanaka, K. Mochizuki, K. Yoshimatsu, T. Sakurai, T. Fujiwara, Purification, characterization, and genetic analysis of Cu-containing dissimilatory nitrite reductase from a denitrifying halophilic archaeon, *Haloarcula marismortui*, J. Bacteriol. 183 (2001) 4149–4156, https://doi.org/10.1128/JB.183.14.4149-4156.2001.
[60] W.G. Zumft, D.J. Gotzmann, P.M. Kroneck, Type 1, blue copper proteins constitute a respiratory nitrite-reducing system in *Pseudomonas aureofaciens*, Eur. J. Biochem. 168 (1987) 301–307, https://doi.org/10.1111/j.1432-1033.1987.tb13421.x.
[61] F.M. Ferroni, J. Marangon, N.I. Neuman, J.C. Cristaldi, S.M. Brambilla, S.A. Guerrero, M.G. Rivas, A.C. Rizzi, C.D. Brondino, Pseudoazurin from *Sinorhizobium meliloti* as an electron donor to copper-containing nitrite reductase: influence of the redox partner on the reduction potentials of the enzyme copper centers, J. Biol. Inorg. Chem. 19 (2014) 913–921, https://doi.org/10.1007/s00775-014-1124-7.
[62] K. Kobayashi, S. Tagawa, Deligeer, S. Suzuki, The pH-dependent changes of intramolecular electron transfer on copper-containing nitrite reductase, J. Biochem. 126 (2) (1999) 408–412.
[63] M. Masuko, H. Iwasaki, T. Sakurai, S. Suzuki, A. Nakahara, Characterization of nitrite reductase from a denitrifier, *Alcaligenes* sp. NCIB 11015. A novel copper protein1, J. Biochem. 96 (1984) 447–454, https://doi.org/10.1093/oxfordjournals.jbchem.a134856.
[64] K. Olesen, A. Veselov, Y. Zhao, Y. Wang, B. Danner, C.P. Scholes, J.P. Shapleigh, Spectroscopic, kinetic, and electrochemical characterization of heterologously expressed wild-type and mutant forms of copper-containing nitrite reductase from *Rhodobacter sphaeroides* 2.4.3, Biochemistry 37 (1998) 6086–6094, https://doi.org/10.1021/bi971603z.
[65] S. Suzuki, K. Yamaguchi, K. Kataoka, K. Kobayashi, S. Tagawa, T. Kohzuma, S. Shidara, H. Iwasaki, Deligeer, Spectroscopic characterization and

intramolecular electron transfer processes of native and type 2 Cu-depleted nitrite reductases, J. Biol. Inorg. Chem. 2 (2) (1997) 265–274.
[66] M.G. Almeida, S. Macieira, L.L. Gonçalves, R. Huber, C.A. Cunha, M.J. Romão, C. Costa, J. Lampreia, J.J.G. Moura, I. Moura, The isolation and characterization of cytochrome *c* nitrite reductase subunits (NrfA and NrfH) from *Desulfovibrio desulfuricans* ATCC 27774. Re-evaluation of the spectroscopic data and redox properties, Eur. J. Biochem. 270 (2003) 3904–3915. 10.1046/j.1432-1033.2003.03772.x.
[67] M.L. Rodrigues, T.F. Oliveira, I.A.C. Pereira, M. Archer, X-ray structure of the membrane-bound cytochrome *c* quinol dehydrogenase NrfH reveals novel haem coordination, EMBO J. 25 (2006) 5951–5960, https://doi.org/10.1038/sj.emboj.7601439.
[68] V.A. Bamford, H.C. Angove, H.E. Seward, A.J. Thomson, J.A. Cole, J.N. Butt, A.M. Hemmings, D.J. Richardson, Structure and spectroscopy of the periplasmic cytochrome *c* nitrite reductase from *Escherichia coli*, Biochemistry 41 (2002) 2921–2931, https://doi.org/10.1021/bi015765d.
[69] T. Tikhonova, A. Tikhonov, A. Trofimov, K. Polyakov, K. Boyko, E. Cherkashin, T. Rakitina, D. Sorokin, V. Popov, Comparative structural and functional analysis of two octaheme nitrite reductases from closely related *Thioalkalivibrio* species, FEBS J. 279 (2012) 4052–4061, https://doi.org/10.1111/j.1742-4658.2012.08811.x.
[70] T.V. Tikhonova, A. Slutsky, A.N. Antipov, K.M. Boyko, K.M. Polyakov, D.Y. Sorokin, R.A. Zvyagilskaya, V.O. Popov, Molecular and catalytic properties of a novel cytochrome *c* nitrite reductase from nitrate-reducing haloalkaliphilic sulfur-oxidizing bacterium *Thioalkalivibrio nitratireducens*, Biochim. Biophys. Acta 1764 (2006) 715–723, https://doi.org/10.1016/j.bbapap.2005.12.021.
[71] M. Kern, J. Simon, Electron transport chains and bioenergetics of respiratory nitrogen metabolism in *Wolinella succinogenes* and other Epsilonproteobacteria, Biochim. Biophys. Acta 1787 (2009) 646–656, https://doi.org/10.1016/j.bbabio.2008.12.010.
[72] J. Simon, Enzymology and bioenergetics of respiratory nitrite ammonification, FEMS Microbiol. Rev. 26 (2002) 285–309, https://doi.org/10.1111/j.1574-6976.2002.tb00616.x.
[73] I.A.C. Pereira, J. LeGall, A.V. Xavier, M. Teixeira, Characterization of a heme *c* nitrite reductase from a non-ammonifying microorganism, *Desulfovibrio vulgaris* Hildenborough, Biochim. Biophys. Acta 1481 (2000) 119–130, https://doi.org/10.1016/s0167-4838(00)00111-4.
[74] M. Kern, J. Volz, J. Simon, The oxidative and nitrosative stress defence network of *Wolinella succinogenes*: cytochrome *c* nitrite reductase mediates the stress response to nitrite, nitric oxide, hydroxylamine and hydrogen peroxide: Stress defence networks in *W. succinogenes*, Environ. Microbiol. 13 (2011) 2478–2494, https://doi.org/10.1111/j.1462-2920.2011.02520.x.
[75] J. Simon, M. Kern, B. Hermann, O. Einsle, J.N. Butt, Physiological function and catalytic versatility of bacterial multihaem cytochromes *c* involved in nitrogen and sulfur cycling, Biochem. Soc. Trans. 39 (2011) 1864–1870, https://doi.org/10.1042/BST20110713.
[76] C.E. Vine, J.A. Cole, Nitrosative stress in *Escherichia coli*: reduction of nitric oxide, Biochem. Soc. Trans. 39 (2011) 213–215, https://doi.org/10.1042/BST0390213.
[77] C. Costa, A. Macedo, I. Moura, J.J.G. Moura, J. Le Gall, Y. Berlier, M.-Y. Liu, W.J. Payne, Regulation of the hexaheme nitrite/nitric oxide reductase of *Desulfovibrio desulfuricans*, *Wolinella succinogenes* and *Escherichia coli*: A mass spectrometric study, FEBS Lett. 276 (1990) 67–70, https://doi.org/10.1016/0014-5793(90)80508-g.
[78] S.R. Poock, E.R. Leach, J.W.B. Moir, J.A. Cole, D.J. Richardson, Respiratory detoxification of nitric oxide by the cytochrome *c* nitrite reductase of *Escherichia coli*, J. Biol. Chem. 277 (2002) 23664–23669, https://doi.org/10.1074/jbc.M200731200.
[79] C.M. Silveira, S. Besson, I. Moura, J.J.G. Moura, M.G. Almeida, Measuring the cytochrome *c* nitrite reductase activity-practical considerations on the enzyme assays, Bioinorg. Chem. Appl. 2010 (2010) 1–8, https://doi.org/10.1155/2010/634597.
[80] P. Stach, O. Einsle, W. Schumacher, E. Kurun, P.M. Kroneck, Bacterial cytochrome *c* nitrite reductase: new structural and functional aspects, J. Inorg. Biochem. 79 (2000) 381–385, https://doi.org/10.1016/s0162-0134(99)00248-2.
[81] J.H. van Wonderen, B. Burlat, D.J. Richardson, M.R. Cheesman, J.N. Butt, The nitric oxide reductase activity of cytochrome *c* nitrite reductase from *Escherichia coli*, J. Biol. Chem. 283 (2008) 9587–9594, https://doi.org/10.1074/jbc.m709090200.
[82] P. Lukat, M. Rudolf, P. Stach, A. Messerschmidt, P.M.H. Kroneck, J. Simon, O. Einsle, Binding and reduction of sulfite by cytochrome *c* nitrite reductase, Biochemistry 47 (2008) 2080–2086, https://doi.org/10.1021/bi7021415.
[83] O. Einsle, A. Messerschmidt, P. Stach, G.P. Bourenkov, H.D. Bartunik, R. Huber, P.M. Kroneck, Structure of cytochrome *c* nitrite reductase, Nature 400 (1999) 476–480, https://doi.org/10.1038/22802.
[84] O. Einsle, P. Stach, A. Messerschmidt, J. Simon, A. Kröger, R. Huber, P.M.H. Kroneck, Cytochrome *c* nitrite reductase from *Wolinella succinogenes*: Structure at 1.6 å resolution, inhibitor binding, and heme-packing motifs, J. Biol. Chem. 275 (2000) 39608–39616. 10.1074/jbc.m006188200.
[85] K.M. Polyakov, K.M. Boyko, T.V. Tikhonova, A. Slutsky, A.N. Antipov, R.A. Zvyagilskaya, A.N. Popov, G.P. Bourenkov, V.S. Lamzin, V.O. Popov, High-resolution structural analysis of a novel octaheme cytochrome c nitrite reductase from the haloalkaliphilic bacterium *Thioalkalivibrio nitratireducens*, J. Mol. Biol. 389 (2009) 846–862, https://doi.org/10.1016/j.jmb.2009.04.037.
[86] T.A. Clarke, A.M. Hemmings, B. Burlat, J.N. Butt, J.A. Cole, D.J. Richardson, Comparison of the structural and kinetic properties of the cytochrome *c* nitrite reductases from *Escherichia coli*, *Wolinella succinogenes*, *Sulfurospirillum deleyianum* and *Desulfovibrio desulfuricans*, Biochem. Soc. Trans. 34 (2006) 143–145, https://doi.org/10.1042/BST0340143.
[87] D. Bykov, F. Neese, Reductive activation of the heme iron-nitrosyl intermediate in the reaction mechanism of cytochrome *c* nitrite reductase: a theoretical study, J. Biol. Inorg. Chem. 17 (2012) 741–760, https://doi.org/10.1007/s00775-012-0893-0.
[88] T.A. Clarke, G.L. Kemp, J.H. Van Wonderen, R.-M.-A.-S. Doyle, J.A. Cole, N. Tovell, M.R. Cheesman, J.N. Butt, D.J. Richardson, A.M. Hemmings, Role of a conserved glutamine residue in tuning the catalytic activity of *Escherichia coli* cytochrome *c* nitrite reductase, Biochemistry 47 (2008) 3789–3799, https://doi.org/10.1021/bi702175w.
[89] C.A. Cunha, S. Macieira, J.M. Dias, G. Almeida, L.L. Gonçalves, C. Costa, J. Lampreia, R. Huber, J.J.G. Moura, I. Moura, M.J. Romão, Cytochrome *c* nitrite reductase from *Desulfovibrio desulfuricans* ATCC 27774: the relevance of the two calcium sites in the structure of the catalytic subunit (NrfA), J. Biol. Chem. 278 (2003) 17455–17465, https://doi.org/10.1074/jbc.m211777200.
[90] C.W.J. Lockwood, T.A. Clarke, J.N. Butt, A.M. Hemmings, D.J. Richardson, Characterization of the active site and calcium binding in cytochrome *c* nitrite reductases, Biochem. Soc. Trans. 39 (2011) 1871–1875, https://doi.org/10.1042/BST20110731.
[91] J. Campeciño, S. Lagishetty, Z. Wawrzak, V. Sosa Alfaro, N. Lehnert, G. Reguera, J. Hu, E.L. Hegg, Cytochrome *c* nitrite reductase from the bacterium *Geobacter lovleyi* represents a new NrfA subclass, J. Biol. Chem. 295 (33) (2020) 11455–11465.
[92] W. Schumacher, U. Hole, P.M. Kroneck, Ammonia-forming cytochrome *c* nitrite reductase from *Sulfurospirillum deleyianum* is a tetraheme protein: new aspects of the molecular composition and spectroscopic properties, Biochem. Biophys. Res. Commun. 205 (1994) 911–916, https://doi.org/10.1006/bbrc.1994.2751.
[93] W. Schumacher, P.M.H. Kroneck, Dissimilatory hexaheme c nitrite reductase of *Spirillum* strain 5175: purification and properties, Arch. Microbiol. 156 (1991) 70–74, https://doi.org/10.1007/bf00418190.
[94] D.J. Eaves, J. Grove, W. Staudenmann, P. James, R.K. Poole, S.A. White, I. Griffiths, J.A. Cole, Involvement of products of the nrfEFG genes in the covalent attachment of haem *c* to a novel cysteine-lysine motif in the cytochrome c_{552} nitrite reductase from *Escherichia coli*: Haem ligation to a cysteine-lysine motif in *E. coli* nitrite reductase, Mol. Microbiol. 28 (1998) 205–216, https://doi.org/10.1046/j.1365-2958.1998.00792.x.
[95] C. Lockwood, J.N. Butt, T.A. Clarke, D.J. Richardson, Molecular interactions between multihaem cytochromes: probing the protein-protein interactions between pentahaem cytochromes of a nitrite reductase complex, Biochem. Soc. Trans. 39 (2011) 263–268, https://doi.org/10.1042/BST0390263.
[96] T.V. Tikhonova, A.A. Trofimov, V.O. Popov, Octaheme nitrite reductases: structure and properties, Biochemistry (Mosc.) 77 (2012) 1129–1138, https://doi.org/10.1134/S0006297912100057.
[97] A.A. Trofimov, K.M. Polyakov, T.V. Tikhonova, A.V. Tikhonov, T.N. Safonova, K. M. Boyko, P.V. Dorovatovskii, V.O. Popov, Covalent modifications of the catalytic tyrosine in octahaem cytochrome *c* nitrite reductase and their effect on the enzyme activity, Acta Crystallogr. D Biol. Crystallogr. 68 (2012) 144–153, https://doi.org/10.1107/S0907444911052632.
[98] T.A. Clarke, J.A. Cole, D.J. Richardson, A.M. Hemmings, The crystal structure of the pentahaem *c*-type cytochrome NrfB and characterization of its solution-state interaction with the pentahaem nitrite reductase NrfA, Biochem. J. 406 (2007) 19–30, https://doi.org/10.1042/BJ20070321.
[99] H. Gao, Z.K. Yang, S. Barua, S.B. Reed, M.F. Romine, K.H. Nealson, J.K. Fredrickson, J.M. Tiedje, J. Zhou, Reduction of nitrate in *Shewanella oneidensis* depends on atypical NAP and NRF systems with NapB as a preferred electron transport protein from CymA to NapA, ISME J. 3 (2009) 966–976, https://doi.org/10.1038/ismej.2009.40.
[100] M. Youngblut, E.T. Judd, V. Srajer, B. Sayyed, T. Goelzer, S.J. Elliott, M. Schmidt, A.A. Pacheco, Laue crystal structure of *Shewanella oneidensis* cytochrome *c* nitrite reductase from a high-yield expression system, J. Biol. Inorg. Chem. 17 (2012) 647–662, https://doi.org/10.1007/s00775-012-0885-0.
[101] M.-C. Liu, C. Costa, I. Moura, [21] Hexaheme nitrite reductase from *Desulfovibrio desulfuricans* (ATCC 27774), in: Methods in Enzymology, Elsevier, 1994: pp. 303–319.
[102] T.A. Clarke, P.C. Mills, S.R. Poock, J.N. Butt, M.R. Cheesman, J.A. Cole, J.C.D. Hinton, A.M. Hemmings, G. Kemp, C.A.G. Söderberg, S. Spiro, J. Van Wonderen, D.J. Richardson, *Escherichia coli* cytochrome *c* nitrite reductase NrfA, Methods Enzymol. 437 (2008) 63–77, https://doi.org/10.1016/S0076-6879(07)37004-3.
[103] M.G. Almeida, C.M. Silveira, B. Guigliarelli, P. Bertrand, J.J.G. Moura, I. Moura, C. Léger, A needle in a haystack: the active site of the membrane-bound complex cytochrome *c* nitrite reductase, FEBS Lett. 581 (2007) 284–288, https://doi.org/10.1016/j.febslet.2006.12.023.
[104] V. Andoralov, S. Shleev, N. Dergousova, O. Kulikova, V. Popov, T. Tikhonova, Octaheme nitrite reductase: The mechanism of intramolecular electron transfer and kinetics of nitrite bioelectroreduction, Bioelectrochemistry 138 (2021), https://doi.org/10.1016/j.bioelechem.2020.107699 107699.
[105] R.-M.-A.-S. Doyle, S.J. Marritt, J.D. Gwyer, T.G. Lowe, T.V. Tikhonova, V.O. Popov, M.R. Cheesman, J.N. Butt, Contrasting catalytic profiles of multiheme nitrite reductases containing CxxCK heme-binding motifs, J. Biol. Inorg. Chem. 18 (2013) 655–667, https://doi.org/10.1007/s00775-013-1011-7.

[106] S.J. Marritt, G.L. Kemp, L. Xiaoe, J.R. Durrant, M.R. Cheesman, J.N. Butt, Spectroelectrochemical characterization of a pentaheme cytochrome in solution and as electrocatalytically active films on nanocrystalline metal-oxide electrodes, J. Am. Chem. Soc. 130 (2008) 8588–8589, https://doi.org/10.1021/ja802641a.
[107] S. Todorovic, M.L. Rodrigues, D. Matos, I.A.C. Pereira, Redox properties of lysine- and methionine-coordinated hemes ensure downhill electron transfer in $NrfH_2A_4$ nitrite reductase, J. Phys. Chem. B 116 (2012) 5637–5643, https://doi.org/10.1021/jp301356m.
[108] J.T. Lin, V. Stewart, Nitrate assimilation by bacteria, Adv. Microb. Physiol. 39 (1998) 1–30, 379. 10.1016/s0065-2911(08)60014-4.
[109] T. Hase, P. Schürmann, D.B. Knaff, The interaction of ferredoxin with ferredoxin-dependent enzymes, in: J.H. Golbeck (Ed.), Advances in Photosynthesis and RespirationPhotosystem I, Springer Netherlands, Dordrecht, 2006, pp. 477–498.
[110] S. Nakano, M. Takahashi, A. Sakamoto, H. Morikawa, K. Katayanagi, Structure-function relationship of assimilatory nitrite reductases from the leaf and root of tobacco based on high-resolution structures, Protein Sci. 21 (2012) 383–395, https://doi.org/10.1002/pro.2025.
[111] F. Ramos, G. Blanco, J.C. Gutiérrez, F. Luque, M. Tortolero, Identification of an operon involved in the assimilatory nitrate-reducing system of *Azotobacter vinelandii*, Mol. Microbiol. 8 (1993) 1145–1153, https://doi.org/10.1111/j.1365-2958.1993.tb01659.x.
[112] C. Pino, F. Olmo-Mira, P. Cabello, M. Martínez-Luque, F. Castillo, M.D. Roldán, C. Moreno-Vivián, The assimilatory nitrate reduction system of the phototrophic bacterium *Rhodobacter capsulatus* E1F1, Biochem. Soc. Trans. 34 (2006) 127–129, https://doi.org/10.1042/BST0340127.
[113] A.J. Gates, V.M. Luque-Almagro, A.D. Goddard, S.J. Ferguson, M.D. Roldán, D.J. Richardson, A composite biochemical system for bacterial nitrate and nitrite assimilation as exemplified by *Paracoccus denitrificans*, Biochem. J. 435 (2011) 743–753, https://doi.org/10.1042/BJ20101920.
[114] M.M. Nakano, T. Hoffmann, Y. Zhu, D. Jahn, Nitrogen and oxygen regulation of *Bacillus subtilis nas*DEF encoding NADH-dependent nitrite reductase by TnrA and ResDE, J. Bacteriol. 180 (1998) 5344–5350, https://doi.org/10.1128/JB.180.20.5344-5350.1998.
[115] S. Chu, D. Zhang, D. Wang, Y. Zhi, P. Zhou, Heterologous expression and biochemical characterization of assimilatory nitrate and nitrite reductase reveals adaption and potential of *Bacillus megaterium* NCT-2 in secondary salinization soil, Int. J. Biol. Macromol. 101 (2017) 1019–1028, https://doi.org/10.1016/j.ijbiomac.2017.04.009.
[116] J.D. Colandene, R.H. Garrett, Functional dissection and site-directed mutagenesis of the structural gene for NAD(P)H-nitrite reductase in *Neurospora crassa*, J. Biol. Chem. 271 (1996) 24096–24104, https://doi.org/10.1074/jbc.271.39.24096.
[117] N.R. Harborne, L. Griffiths, S.J.W. Busby, J.A. Cole, Transcriptional control, translation and function of the products of the five open reading frames of the *Escherichia coli* nir operon, Mol. Microbiol. 6 (1992) 2805–2813, https://doi.org/10.1111/j.1365-2958.1992.tb01460.x.
[118] Q. Song, B. Wang, F. Zhao, Y. Han, Z. Zhou, Expression, characterization and molecular docking of the assimilatory NADH-nitrite reductase from *Acidovorax wautersii* QZ-4, Biochem. Eng. J. 159 (2020), https://doi.org/10.1016/j.bej.2020.107589 107589.
[119] X. Wang, D. Tamiev, J. Alagurajan, A.A. DiSpirito, G.J. Phillips, M.S. Hargrove, The role of the NADH-dependent nitrite reductase, Nir, from *Escherichia coli* in fermentative ammonification, Arch. Microbiol. 201 (2019) 519–530, https://doi.org/10.1007/s00203-018-1590-3.
[120] J.M. Vega, R.H. Garrett, Siroheme: a prosthetic group of the *Neurospora crassa* assimilatory nitrite reductase, J. Biol. Chem. 250 (1975) 7980–7989, https://doi.org/10.1016/s0021-9258(19)40804-1.
[121] U. Swamy, M. Wang, J.N. Tripathy, S.-K. Kim, M. Hirasawa, D.B. Knaff, J.P. Allen, Structure of spinach nitrite reductase: implications for multi-electron reactions by the iron-sulfur:siroheme cofactor, Biochemistry 44 (2005) 16054–16063, https://doi.org/10.1021/bi050981y.
[122] M.J. Murphy, L.M. Siegel, Siroheme and sirohydrochlorin - the basis for a new type of porphyrin-related prosthetic group common to both assimilatory and dissimilatory sulfite reductases, J. Biol. Chem. 248 (1973) 6911–6919, https://doi.org/10.1016/s0021-9258(19)43436-4.
[123] F. Sulc, P.J. Farmer, Bioinorganic chemistry of the HNO Ligand, in: A. Ghosh (Ed.), The Smallest Biomolecules: Diatomics and Their Interactions with Heme Proteins, Elsevier, 2008, pp. 429–462.
[124] M.E. Stroupe, E.D. Getzoff, in: Tetrapyrroles, Springer New York, New York, NY, 2009, pp. 375–389.
[125] B.R. Crane, L.M. Siegel, E.D. Getzoff, Sulfite reductase structure at 1.6 Å: Evolution and catalysis for reduction of inorganic anions, Science 270 (1995) 59–67. 10.1126/science.270.5233.59.
[126] B.R. Crane, L.M. Siegel, E.D. Getzoff, Probing the catalytic mechanism of sulfite reductase by X-ray crystallography: structures of the *Escherichia coli* hemoprotein in complex with substrates, inhibitors, intermediates, and products, Biochemistry 36 (1997) 12120–12137, https://doi.org/10.1021/bi971066i.
[127] R. Schnell, T. Sandalova, U. Hellman, Y. Lindqvist, G. Schneider, Siroheme- and $[Fe_4\text{-}S_4]$-dependent NirA from *Mycobacterium tuberculosis* is a sulfite reductase with a covalent Cys-Tyr bond in the active site, J. Biol. Chem. 280 (2005) 27319–27328, https://doi.org/10.1074/jbc.M502560200.
[128] M.G. Guerrero, J.M. Vega, M. Losada, The assimilatory nitrate-reducing system and its regulation, Annu. Rev. Plant Physiol. 32 (1981) 169–204, https://doi.org/10.1146/annurev. pp. 32.060181.001125.
[129] A. Herrero, E. Flores, J. Imperial, Nitrogen Assimilation in Bacteria, in: T.M. Schmidt (Ed.), Encyclopedia of Microbiology, 4th Edition, Elsevier, 2019.
[130] J.R. Lancaster, J.M. Vega, H. Kamin, N.R. Orme-Johnson, W.H. Orme-Johnson, R.J. Krueger, L.M. Siegel, Identification of the iron-sulfur center of spinach ferredoxin-nitrite reductase as a tetranuclear center, and preliminary EPR studies of mechanism, J. Biol. Chem. 254 (1979) 1268–1272, https://doi.org/10.1016/s0021-9258(17)34197-2.
[131] M. Hirasawa, G. Tamura, Ferredoxin-dependent nitrite reductase from spinach leaves, Agric. Biol. Chem. 44 (1980) 749–758, https://doi.org/10.1080/00021369.1980.10864029.
[132] M. Hirasawa, G. Tollin, Z. Salamon, D.B. Knaff, Transient kinetic and oxidation-reduction studies of spinach ferrodoxin: nitrate oxidoreductase, Biochim. Biophys. Acta Bioenerg. 1185 (1994) 336–345, https://doi.org/10.1016/0005-2728(94)90249-6.
[133] S. Kuznetsova, D.B. Knaff, M. Hirasawa, P. Sétif, T.A. Mattioli, Reactions of spinach nitrite reductase with its substrate, nitrite, and a putative intermediate, hydroxylamine, Biochemistry 43 (2004) 10765–10774, https://doi.org/10.1021/bi048826r.